

FIG. 1. The 5' and 3' ends of a functional domain of DLS. (A) A schematic image of monomer formation of the E/DLS duplicated mutant (DD-mutant) genome. Genomes of the WT virus form dimers, whereas those of DD-mutant form both dimers and monomers. Solid lines and open circles represent viral genome RNA and E/DLS, respectively. (B) Possible two-dimensional folds of the inserted fragment of each of the constructed mutants. nt., nucleotide. (C) Virion RNA profiles in native agarose gel. Viruses were prepared by transfection of 293T cells with pNLN_h (WT) or its derivative mutants. At 48 h posttransfection, culture supernatants were harvested. Virions in the supernatant were collected by ultracentrifugation through a 20% sucrose cushion for isolation of the virion RNA. Open and solid arrowheads denote positions of dimers and monomers, respectively.

U5/LF (5'-TCTGTTGTGACTCTGGTAAC-3') and the antisense primer SL4Rs. The three amplified fragments were isolated and ligated in pGEM-Teasy (Promega, Madison, WI) to generate pGEMT4sub, pGEMU4sub, and pGEML4sub, respectively. The digestion of these plasmids with EcoRI, blunt ended by T4 DNA polymerase, resulted in the isolation of approximately 300-bp fragments, including the 5' leader region of HIV-1. These fragments were then ligated into the T4 DNA polymerase-treated NheI site of pNL4-3 to construct pDDNT4, pDDNU4, and pDDNL4, respectively. The orientation of the inserted fragments was verified by sequencing. pDDNLp4 and pDDNL4e were constructed in a similar way, except for the use of pDLA3 (39) as a PCR template and different sense primers. The sense primer for pDDNLp4 was A3F+N (5'-TGTGCCGTCTGTTGTGTGACTC-3'), and that for pDDNL4e was A3U5endN (5'-AGTAGTGTGTGCCGTCTGTTGTGTGACTC-3'). To construct pDDNLp4Δ1 and pDDNLp4Δ3, pDM and pDX (25) were used as templates for PCR amplification with the sense primer LpLA3 (5'-TGTGCCGTCTGTTGTGTGACTCTGGTCCAGAGGAG-3') and the antisense primer SL4Rs, respectively. The two amplified fragments were isolated and ligated in pGEM-Teasy to generate pGEMLp4Δ1sub and pGEMLp4Δ3sub, respectively. To construct pDDNLp4Δ2, two-step PCR amplification was performed by using pGEMLp4sub as a template. The first pair of primers comprised the sense primer A3F+N and the antisense primer dS2R (5'-CAAATTTTGGCCCTC GCC-3'), and the second pair comprised the sense primer dS2F (5'-GGCGAG GGGCAAAAATTTTG-3') and the antisense primer SL4Rs. Two amplified fragments were isolated, mixed, and used for the second PCR with primers

A3F+N and SL4Rs to generate a mutated fragment. This fragment was then isolated and ligated in pGEM-Teasy to generate pGEMLp4Δ2sub. To construct pDDNLp4Δ4, pGEMLp4sub was used as a template for PCR amplification with the sense primer A3F+N and the antisense primer dS4 (5'-CATCTCTCCTTC TAGCC-3'). The amplified fragment was isolated and ligated in pGEM-Teasy to generate pGEMLp4Δ4sub. The digestion of pGEMLp4Δ1sub, -Δ2sub, -Δ3sub, and -Δ4sub with EcoRI, blunt ended by T4 DNA polymerase, resulted in the isolation of fragments, including the 5' leader region of HIV-1. These fragments were then ligated into the T4 DNA polymerase-treated NheI site of pNL4-3 to construct pDDNLp4Δ1, -Δ2, -Δ3, and -Δ4, respectively. The EcoRI fragment from pGEMLp4Δ2sub (fragment Lp4Δ2) was blunt ended by T4 DNA polymerase and ligated into the BsaBI site of pDDNLp4Δ2 to create pDTNLp4Δ2. The plasmid p5'ssβglob (24) features a deletion on the 5' untranslated region of pMSMBA (nucleotides 694 to 783) and an insertion at the point of deletion of a portion of the sequence spanning the 5' splicing signal of the first intron of the β-globin gene. The 2.2-kb StuI-XhoI fragments containing env regions of pDDNLp4Δ2 and pDTNLp4Δ2 were inserted into the corresponding position of p5'ssβglob to create pssNLp4Δ2 and psTNLp4Δ2, respectively. The fragment Lp4Δ2 was blunt ended by T4 DNA polymerase and ligated into the T4 DNA polymerase-treated XhoI site of pNL4-3 to construct pDDEX+. The fragment Lp4Δ2 was ligated into the EcoRI site of pNL4-3 to construct pDDEE+. pDDEE+ was digested with Sse8387I, and NheI, a 4.4-kb, *pol-env* region-containing fragment, was isolated and exchanged at the same position of pDDEX+ to construct pDTEXE+. The construction of the HIV-2 env expression vector, pCGH2env, has been described previously elsewhere (28).

DNA transfection. 293T cells (13) (approximately 3×10^6) were seeded on dishes (diameter, 100 mm) the day before transfection with plasmid DNA (5 μg) by means of the calcium phosphate precipitation method (3). The day after transfection, the supernatant was replaced with fresh medium.

Virus infection. At 48 to 72 h posttransfection, the medium was centrifuged and the supernatant was used for infection with inoculation of equal amounts of CA-p24 into MT-4, M8166, or M8166/H1Luc cells (27). The supernatants of MT-4 or M8166 were harvested every 3 or 4 days for the multiple replication assay, while 10 μl of each cell supernatant was analyzed with the exogenous reverse transcriptase (RT) assay as described previously (43). M8166/H1Luc cells contain integrated reporter DNA carrying the HIV-1 LTR and luciferase. Upon infection with HIV-1, the HIV-1 LTR is activated along with the expression of viral transactivator Tat and luciferase expression in cytoplasm is induced. The same amount of CA-p24 recovered from each construct was inoculated into M8166/H1Luc cells, and luciferase expression within the cells was measured 24 h after infection. The luciferase assay was performed with the Bright-Glo luciferase assay system (Promega).

Isolation of RNA from virions. At 48 to 72 h posttransfection, virus particles were collected concurrently from medium as described previously elsewhere (23). The physical virus titer was determined with an enzyme-linked immunosorbent assay kit to quantitate CA-p24 (ZeptoMetrix, Inc., Buffalo, NY). To isolate RNA from particles, virions were disrupted by the addition of 1% sodium dodecyl sulfate and treated with proteinase K (300 μg/ml) at room temperature for 60 min, followed by Tris-EDTA-saturated phenol-chloroform extraction, chloroform extraction, and ethanol precipitation.

Northern blotting analysis. Pelleted RNA was resuspended in T buffer (10 mM Tris-HCl, pH 7.5, 1 mM EDTA, 1% sodium dodecyl sulfate, 100 mM NaCl, and 10% formamide), and the thermostability of dimeric viral RNA was determined by incubating RNA aliquots for 10 min at the temperatures indicated (42). RNA electrophoresis on native agarose gel and Northern hybridization analysis were performed as described previously elsewhere (41). Plasmid T7pol (42) was used to synthesize a cRNA probe for Northern hybridization. In experiments designed to assess the conversion of dimers to monomers, relative amounts of both RNA species were quantitated by PhosphorImager analysis (Fujifilm Co., Tokyo, Japan) and ratios of dimers and monomers were determined.

RNAse protection assay. The antisense probe ($\sim 10^8$ cpm/mg) specific to the NL4-3 *gag* region was synthesized by *in vitro* transcription. One-fifth of the virion-associated RNA was mixed with 8×10^4 Cerenkov counts of 32 P-labeled antisense riboprobe and precipitated with ethanol. RNAse protection assays were performed with an RPA III RNAse protection assay kit (Ambion, Inc., Austin, TX). After electrophoresis in 5% polyacrylamide-8 M urea gels, protected RNA was quantitated by PhosphorImager analysis (Fujifilm Co.).

Real-time PCR analysis. At 48 to 72 h posttransfection, culture supernatants of the transfected cells were harvested. The supernatants were treated with DNase prior to infection to eliminate plasmid DNA contamination as described previously elsewhere (20) and inoculated into 10^6 MT-4 cells. For PCR analysis, total DNA was extracted from infected cells 20 h after infection by using a GenElute mammalian genomic DNA miniprep kit (Sigma, St. Louis, MO).

TABLE 1. Packaging efficiency of the mutants analyzed^a

Mutant or WT	Avg ± SEM
WT.....	1 ± 0
DDNT4.....	0.84 ± 0.14
DDNU4.....	1.61 ± 0.26
DDNL4.....	1.09 ± 0.10
DDNLp4.....	1.04 ± 0.08
DDNL _e 4.....	0.94 ± 0.09

^a The values were calculated by dividing the quantity of viral RNA by that of CA-p24. The value of WT (NLN_h) was set at 1. Values are averages of results of at least three independent experiments.

Real-time PCR was performed with an Applied Biosystems 7500 real-time PCR system to quantitate viral cDNA synthesis during infection. Primers and TaqMan probes were selected according to criteria described previously elsewhere (19), and samples (0.5 µg DNA) were subjected to 40 cycles of PCR in a 10-µl reaction mixture. A series of known amounts of plasmid DNA were amplified along with total DNA to serve as a standard in each experiment. For the quantitation of the 2-LTR from virus DNA, a 2-LTR circle junction was cloned into pGEM-Teasy plasmid (Promega) as a TA cloning fragment by PCR amplification from 2-LTR circles, with total DNA extracted from infected MT-4 cells serving as a template. Serial dilutions of this plasmid were used as a standard to determine copy numbers of 2-LTR circles in the samples in the same manner as that for the determination of other DNA copy numbers.

For integrated proviral DNA quantitation, a modification of a recently reported Alu PCR method (7, 18) was employed (28). In short, two outward-facing Alu primers that anneal within the conserved regions of the Alu repeat element were used, together with an HIV-1 LTR-specific primer (L-M667), to optimize the probability of amplifying an LTR sequence for the first round of PCR. For the second round of PCR (real-time PCR), a lambda-specific primer (Lambda T) was used as a sense primer to detect only the amplified fragments in the first round of PCR and a TaqMan probe and an antisense primer were selected from the previous set for R/U5 DNA detection (19). The resultant PCR products were diluted 100-fold and subjected to real-time PCR.

RESULTS

The 5' and 3' ends of a functional domain of DIS/DLS. In a previous study of ours, the minimal RNA region required for RNA dimerization in virions was identified as a fragment inserted in the *env* region of pDDNBA (41). The fragment was approximately 500 bases long, extending from the 5' capping site to the middle of the MA gene of the viral genome with deletion of the polyadenylation signal and primer binding site (PBS). We first

constructed five mutants to precisely map the 5' and 3' ends of the functional region of DIS/DLS (Fig. 1). The viral genome packaging efficiency of all mutants was similar to that of the wild type (WT), indicating that the mutations had little effect on packaging ability (Table 1). The viral genome from mutant DDNT4, which contains an ectopic fragment (334 bases, from the *trans*-acting responsive element [TAR] to SL4) at the *env* region, formed a monomer very similar to that of the original mutant DDNBA (monomer content was more than 40% of the total viral genome in native condition), which indicated that sequence 3' to SL4 was not needed for mediating RNA-RNA interactions in virions (data not shown). pDDNU4 carried a fragment from the R/U5 [poly(A)] stem-loop to SL4 (277 bases), and pDDNL4 carried a fragment from the U5/L stem-loop to SL4 (222 bases). As shown in Fig. 1B, the viral genome from DDNU4 formed a monomeric RNA comparable to DDNBA (monomer content was more than 40%), whereas the viral genome from DDNL4 formed a monomeric RNA with a greatly reduced amount of monomer (<20%). These results indicate that the 5' end of the functional region of DIS/DLS was lost from DDNL4. We therefore added 8 and 15 nucleotides of the 5' sequences to DDNL4 to generate DDNLp4 and DDNL_e4, respectively. An upper stem-loop and PBS of the U5/L region were deleted from the inserted fragment of DDNLp4 and DDNL_e4 because our previous data showed that those parts were dispensable for the dimer linkage formation function (41). Both viral RNAs of DDNLp4 and DDNL_e4 formed a genome with a monomeric content (>40%) comparable to that of the WT in the virion (Fig. 1B). Taken together, these findings suggest that the region from the R/U5-U5/L junction to SL4 is sufficient to produce dimeric RNA in virions.

Minimal region sufficient for RNA dimerization is 144 bases long. We then examined the involvement in dimer linkage formation of four stem-loops, SL1 (putative "DIS"), SL2 (splicing signal), SL3 (essential region of packaging signal), and SL4 (containing *gagAUG*). Four mutants, DDNLp4Δ1, DDNLp4Δ2, DDNLp4Δ3, and DDNLp4Δ4, were constructed as derivatives of DDNLp4. Each mutant contained a deletion of one of four stem-loops on the ectopic fragment of DDNLp4 (Fig. 2A). As shown in Fig. 2B, only DDNLp4Δ2 formed a monomeric genome similar to the one derived from DDNBA,

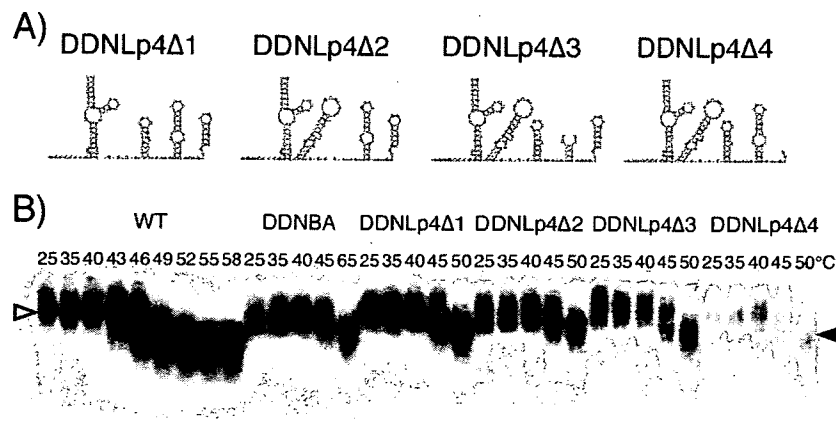


FIG. 2. Determination of the necessary and sufficient DLS in virions. (A) Probable two-dimensional folds of the inserted fragment of each of the constructed mutants. (B) Virion RNA profiles in native agarose gel. Virion RNA was isolated, and Northern hybridization was performed as described for Fig. 1. Open and solid arrowheads denote positions of dimers and monomers, respectively.

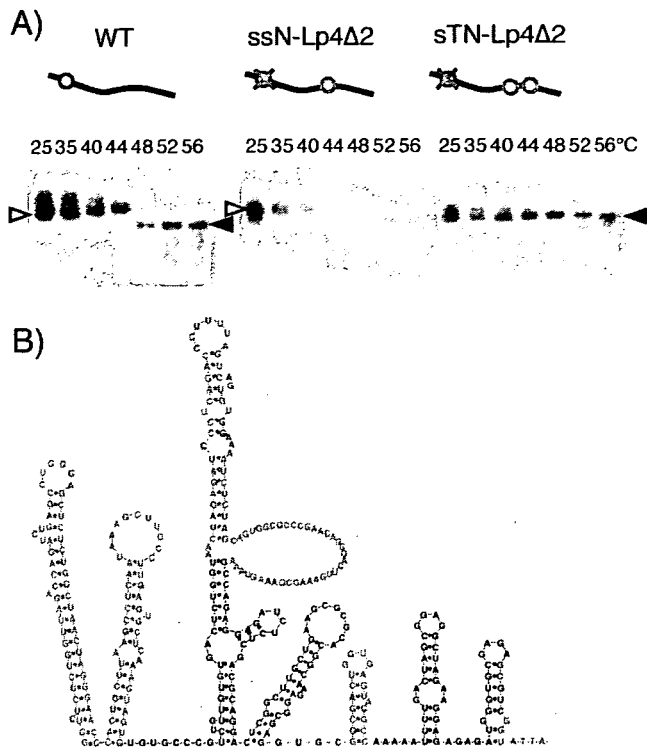


FIG. 3. Verification of the minimal DLS for its ability to induce RNA-RNA interaction in HIV-1 virions. (A) Virion RNA profiles in native agarose gel. Virion RNA was isolated, and Northern hybridization was performed as described for Fig. 1. Open and solid arrowheads denote positions of dimers and monomers, respectively. Schematic diagrams of mutants are shown above the blots. Solid lines, open circles, gray circles, and gray crosses represent viral genome RNA, authentic E/DLS, Lp4 Δ 2 fragments, and mutations introduced to knock out E/DLS functions, respectively. (B) A schematic Mfold representative of the verified area.

whereas other mutants displayed low levels of monomeric genome formation in virions. This indicates that the major splicing donor, SL2, is dispensable for RNA-RNA interaction, while the three other stem-loops are necessary for dimer linkage formation in virions.

In a previous study, we constructed two mutants, ssN $-$ and sTN $-$, which contained a deletion of authentic DIS/DLS and an insertion of one (ssN $-$) or two (sTN $-$) DIS/DLS fragments in the ectopic position of the viral genome (39). Viral genomes from dimers formed from ssN $-$ were similar to the WT, and nearly all viral genomes in virions of sTN $-$ were monomers. This suggests that the two fragments inserted on one RNA strand interacted exclusively and intramolecularly with each other to prevent intermolecular dimerization. To confirm that fragment Lp4 Δ 2 was necessary and sufficient for RNA dimer linkage formation in virions, we constructed two mutants, ssNLp4 Δ 2 and sTNLp4 Δ 2, in the same way that ssN $-$ and sTN $-$ were constructed, except for the use of fragment Lp4 Δ 2 for insertion. As we expected, viral genomes from ssNLp4 Δ 2 formed dimers similar to those of the WT, while the viral genome from sTNLp4 Δ 2 exclusively formed monomers (Fig. 3A). Thus, the Lp4 Δ 2 fragment, 144 bases in length, was nec-

essary and sufficient for mediating RNA dimerization in HIV-1 virions (Fig. 3B).

Single-round infection efficiency of HIV-1 mutant containing monomeric genome. We previously demonstrated the particle formation of HIV-1 which contained exclusively monomeric genome (39). This suggested that whole-genome dimerization is not essential for RNA packaging and particle formation of the viral genome, although dimer linkage formation of the DLS region is essential for these functions (41). On the other hand, no efficient infection or replication of HIV-1 mutants containing a monomeric genome was observed since significant reduction of intact viral DNA production occurred as a result of aberrant strand transfer and/or recombination during reverse transcription (39). Strand transfer during the reverse transcription process of the retroviral genome targets the R region of the viral LTR (12), which has also been suggested to be a hot spot for recombination (26). The production of aberrant viral cDNA products could thus be induced by the presence of multimerized R regions on the genome of the mutants. Since Lp4 Δ 2, the minimum DLS we identified here, did not include any R region, its ability to induce aberrant strand transfer and/or recombination by duplication of Lp4 Δ 2 in the viral genome was expected to be reduced. We therefore compared the single-round replication efficiencies of mutants DDNLp4 Δ 1, $-\Delta$ 2, $-\Delta$ 3, and $-\Delta$ 4 pseudotyped with the HIV-2 envelope. The result demonstrated that all mutants containing Lp4 fragments showed reduced infectivity, which may be the effect of homologous recombination at a sequence-duplicated location (Fig. 4A). However, the infectivity of DDNLp4 Δ 2, the only mutant packaging monomeric genome, was three- to five-fold lower than that of other mutants. As the M8166/H1Luc cell assay reflects the magnitude of Tat expression of the samples, this result suggests that the mutations introduced in these constructs affect mainly the step(s) between virus penetration and early gene expression.

Reverse transcription predominantly blocked in monomeric genome mutants. To determine the step(s) in the viral replication cycle affected by the mutation described above, we analyzed the efficiency of each of the replication steps of the mutants. We chose two mutants, DDNLp4 Δ 2 and $-\Delta$ 3, for comparison, since they are very similar in length of duplicated sequences but quite different in infectivity. We analyzed the virion production and viral RNA encapsidation ability of the mutants by purifying the virion and viral RNA from the supernatant of transfectant 293T cells. As shown in Fig. 4B, both functions of the mutants were similar or only moderately reduced compared to those of the WT, indicating that the mutations had little effect on these processes.

We next quantitated the levels of virus reverse-transcribed products, 2-LTR viral circular DNA, and integrated viral DNA using real-time PCR. HIV-2 *env*-pseudotyped virus was generated by transfection and purified, and equivalent amounts of CA-p24 were used to infect MT-4 cells. At 20 h after infection, total DNA was isolated from virus-infected cells. To examine the progress of reverse transcription, four sets of primers and probes were prepared (see Materials and Methods) and used to measure the synthesis of the strong-stop negative-strand DNA, first-strand transferred DNA, *gag* region DNA, and second-strand transferred DNA within total cellular DNA. Figure 4C shows the organized results of viral DNA quantitation.

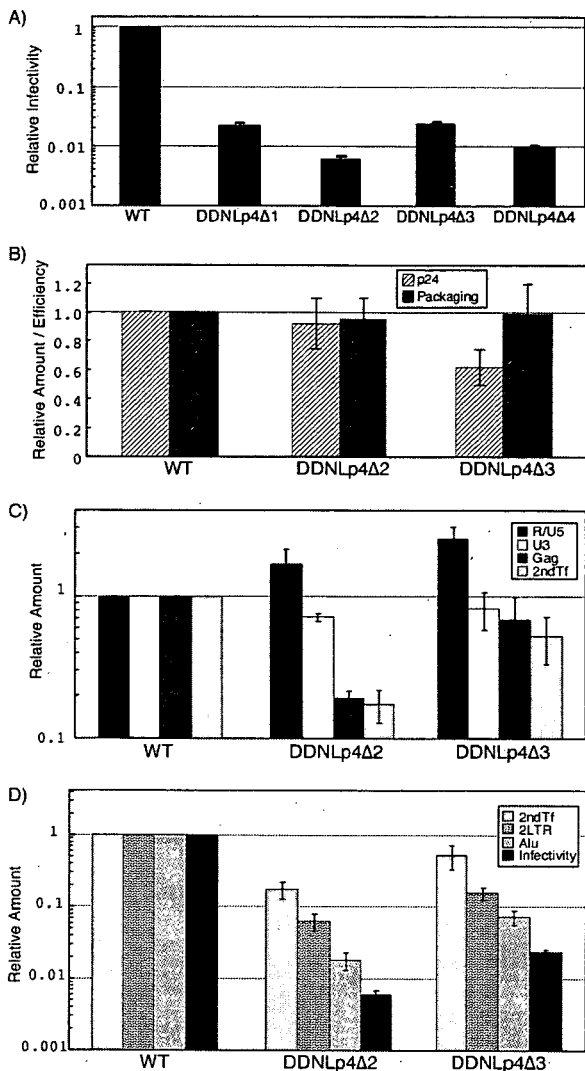


FIG. 4. Infectivity of mutant viruses. For each graph, the value of the WT was set at 1. Figures show the averages of results of at least two independent experiments. Error bars represent standard errors. (A) Single-round replication assay. M8166/H1Luc cells (1×10^6) were infected with the same quantity of CA-p24 of WT or mutant viruses pseudotyped with HIV-2 Env. At 24 to 48 h postinfection, cells were lysed and luciferase activity in the cell lysate was measured. (B) CA-p24 production and RNA packaging ability. Quantities of CA-p24 and viral RNA of purified virions were measured with the enzyme-linked immunosorbent assay and the RNase protection assay, respectively. Packaging efficiency was calculated by dividing the quantity of viral RNA by that of CA-p24. (C and D) Viral DNA quantification at early infection steps. A total of 1×10^6 MT-4 cells were infected with the same quantity of CA-p24 of WT or mutant viruses pseudotyped with HIV-2 Env. At 20 h postinfection, total cellular DNA was extracted and treated with DpnI overnight to digest methylated plasmid DNA. An equal amount of DNA was subjected to real-time PCR analysis. R/U5, strong-stop DNAs; U3, first-strand transferred products; Gag, negative-strand late products; 2ndTf, second-strand transferred products; 2LTR, 2-LTR viral circular DNA; Alu, PCR quantification for integrated proviral DNA; Infectivity, M8166/H1Luc cell assay as described for Fig. 4A.

Compared to the WT, a moderately large amount of DNA of both mutants was observed at the point of strong-stop DNA synthesis, which was reduced to a level similar to that of the WT in the subsequent first-strand transfer. At the next step, a

big difference between the two mutants was observed. During the elongation of negative-strand DNA, the level of DNA synthesis of the DDNLp4Δ2 mutant was reduced to about 20%, whereas that of the DDNLp4Δ3 mutant remained at more than 60%. The level of DNA after the second-strand transfer showed additional moderate reduction for both of the mutants. As a result, a less than 50% reduction in overall viral cDNA production was observed in the DDNLp4Δ3 mutant, but a more than 80% reduction was observed in the DDNLp4Δ2 mutant. This result suggests that one of the defects was present at the reverse transcription stage. The reduction of the amounts of 2-LTR DNA, integrated DNA, and the infectivity are essentially similar between two mutants (Fig. 4D). As the 2-LTR circular DNA can be used as an indicator of RT completion and nuclear import of viral DNA (19), our findings suggest that the replication process from nuclear import to early gene expression was not specifically affected in a dimerization-defective mutant.

Attempt to generate replication-competent HIV-1 mutant containing monomeric genome. Multi-round replication of a defective mutant virus sometimes results in the appearance of compensatory mutations to recover infectivity of the mutant without affecting viral RNA stability (38). Although we could not detect any efficient infectivity of mutant DDNLp4Δ2, we thought it might be possible to generate a replication-competent HIV-1 mutant containing a monomeric genome by means of long-term culture of infected cells. To verify this possibility, we constructed three mutants with Lp4Δ2 fragments on their genome, which retained all essential genes (*gag*, *pol*, *env*, *tat*, and *rev*) and important accessory genes (*vif* and *vpu*) but packaged the monomeric genome. Fragment Lp4Δ2 was inserted into *vpr*, *nef*, or both of pNL4-3 to construct pDDEE+, pDDXE+, and pDTEXE+, respectively (Fig. 5A). 293T cells were transfected with these constructs, the culture supernatants were harvested 2 to 3 days later, and the released virions collected. Roughly, the level of virion production by all three mutants was similar to that of the WT (data not shown). The genome from mutant virions contained 30 to 50% of monomeric genomes as shown by native Northern blotting analysis, thus confirming our previous observation (Fig. 5C). The mutants were examined for their ability to replicate in human CD4⁺ cell lines MT-4 and M8166. Figure 6B shows the growth kinetics of the mutants in MT-4 cells. Mutant DTEXE+ was replication defective in MT-4 cells, while two mutants, DDEE+ and DDXE+, showed detectable virus replication but with growth kinetics that were significantly reduced and delayed compared to those of WT. On the other hand, all mutants were replication negative in M8166 cells (data not shown). Replicated viruses in the culture supernatant of MT-4 were harvested at their kinetic peak point. Equal amounts of RT units of virus samples were used for assay of reinfection of MT-4 cells, the remainder was centrifuged to purify virions, and the viral genome RNA was isolated. Growth kinetics of reinfected mutants restored their replication ability to a level comparable to that of the WT, suggesting that they had become revertants (data not shown). The results of native Northern blotting of genome RNA showed that MT-4 replicating mutants formed mostly dimers similar to that of the WT (Fig. 5D). Proviral genome sequencing from infected MT-4 chromosomal DNA proved that Lp4Δ2 sequences inserted in ectopic positions of the genome

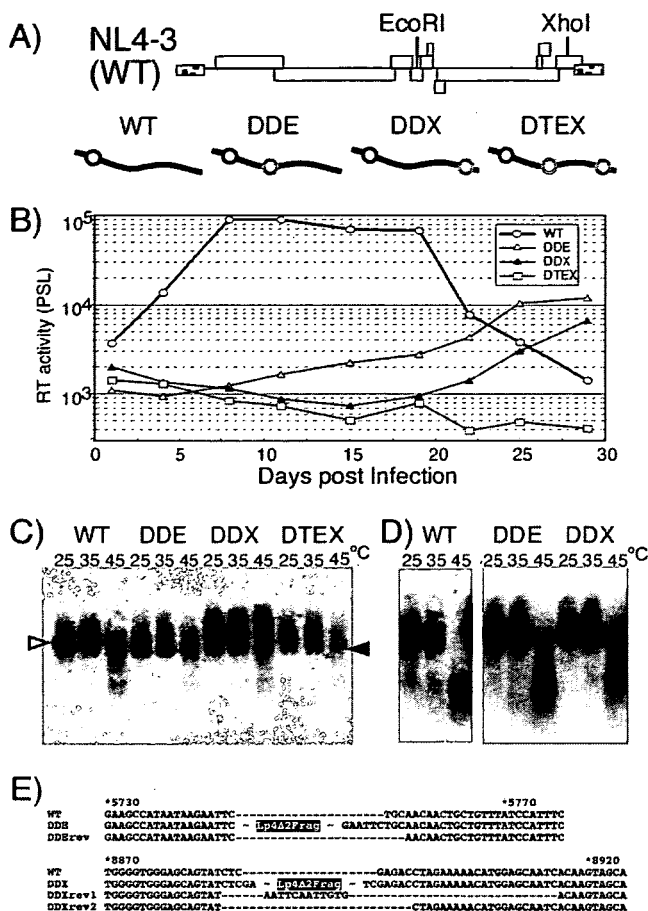


FIG. 5. Replication assay of mutants carrying a monomeric genome. (A) Schematic diagrams of replication-competent form mutants. The positions of restriction enzyme sites on the viral genome used for insertion are shown in the upper part of the panel. Diagrams of the mutants are shown in the lower part of the panel. Symbols are the same as those described for Fig. 3. (B) Growth kinetics of viruses. Values are representative of the results of at least three independent experiments. Viruses were prepared by transfection of 293T cells with pNL4-3 (WT) or its derivative mutants (pDDEE+ [DDE], pDDXE+ [DDX], and pDTEXE+ [DTE]). At 48 h posttransfection, culture supernatants of transfected 293T cells were harvested, and equal quantities of CA-p24 were inoculated into MT-4 cells. The supernatants of the cells were harvested every 3 or 4 days. Ten microliters of each cell supernatant was subjected to exogenous RT assay and quantitated by PhosphorImager analysis. PSL, Photostimulierte Lumineszenz. (C) Virion RNA profiles produced from transfected 293T cells and visualized by native Northern blotting analysis. Open and solid arrowheads denote positions of dimers and monomers, respectively. (D) Virion RNA profiles produced from MT-4 cells. Viruses were harvested at their growth kinetic peak point (wild type, 10 days postinfection; DDE and DDX, 28 days postinfection). (E) The nature of reversions. The sequences in the vicinity of the fragment-inserted sites are shown. The names of revertant sequences include "rev." The positions of Lp4Δ2 fragment insertion of DDE and DDX are indicated. The numbers above the sequences represent nucleotide positions of pNL4-3 (WT).

were completely deleted from both replication-competent mutants (Fig. 5E). Since the sequences of the revertants were found to contain an additional deletion or a small part of the inserted sequence at the mutated positions (Fig. 5E), the possibility of WT virus contamination could be ruled out.

DISCUSSION

The recent growth in interest in retrovirus genome dimerization has resulted in many publications that deal with its various aspects and that vary in depth and breadth (for reviews, see references 31, 35, and 37). Nonetheless, the overall picture of the retroviral dimerization signal remains unclear, so that there is still a need for detailed examination. The aim of the study reported here was to identify the minimal region sufficient for genome dimerization of HIV-1 in virions. In the first set of experiments, we defined the region sufficient for dimer linkage formation, and, in a subsequent experiment, we generated several deletion mutants to determine the minimal DLS required for HIV genome dimer linkage formation in virions. The minimal DLS identified in this study was only 144 bases long and included SL1, SL3, and SL4. Especially, SL1 deletion is more deleterious than is deletion of the other elements for dimer linkage formation in Fig. 2. It has been suggested that the hairpin loop of SL1 in DLS, known as DIS, plays a crucial role in dimerization and recombination (9, 33, 41). Our findings are well consistent with this notion.

While there are many functional regions for viral viability in the 5' UTR of HIV, such as TAR, polyadenylation signal, PBS, and splicing donor, none was required for the dimerization function. This suggests that the genome dimerization of HIV-1 is independent of transactivation, splicing, or primer annealing. As we pointed out in a previous paper of ours (41) and in this study, the lower stem of the U5/L stem-loop is required for dimerization, which was not clearly identified during *in vitro* studies (for a review, see reference 30). This stem contains a so-called primer activation signal (5), which is thought to activate the initiation of reverse transcription. Since PBS or primer annealing is not required for dimerization, the involvement of primer activation signal and its opposing stem sequence in dimerization may be limited simply to creating a stable structure. Several studies have suggested that TAR, the R-U5 stem-loop region or coding region of *gag*, participates in the dimerization (4, 14, 16, 32). The contribution of those regions to RNA dimerization was demonstrated mainly in *in vitro* assays, but they were not included in the DLS identified in the *in vivo* assay used in our study. However, the possibility of a contribution by these regions cannot be ruled out since all mutants in our study retained the intact 5' UTR. This result means that all mutants possess at least one set of the regions in the original position per genome, so that they may perform certain incidental functions for dimerization in virions.

Mfold RNA stability calculation (44) showed that the junction between R/U5 and U5/L stem-loops is relatively "free," which suggests that it is not involved in a base-pairing interaction with vicinal sequences (Fig. 1A). However, recent reports have suggested that the HIV-1 genome leader region could form an alternative structure known as the branched multiple hairpin (BMH) (1, 17). In this model, the 5' junction sequence forms a stem structure with a sequence at the 3' end of DLS. Although the BMH model was validated in an *in vitro* experiment, the DLS we defined *in vivo* was found to include all sequences required for the BMH formation. As an interaction between 5' and 3' ends of DLS should be essential for BMH formation, we evaluated the importance of both ends *in vivo* by making several base substitution mutants. The mutants con-

tained four to eight-base substitutions in either or both ends of the Lp4Δ2 fragment inserted in pDDNLp4Δ2. As expected, the 5' or 3' region of DLS appeared to be very important in dimer linkage formation of RNA since at least four-base substitutions (four substitutions in 8 bases of the 5' end or four substitutions in 15 bases of the 3' end) seriously disrupted the function (data not shown). Nonetheless, our attempt failed to yield a clear answer to whether BMH structure exists in virion RNA, probably because of difficulty in estimating the effect of the mutations on actual RNA shape in this region.

A noteworthy result of the M8166/H1Luc cell assay, an infectivity assay of monomeric genome mutants, was that the overall single-round infectivity of the mutant DDNLp4Δ2 was dramatically reduced (Fig. 4A). In our previous study, we reported that another monomeric genome mutant, DDNLp4Δ3, produced virions with less than 1% of infectivity of the WT (in one representative experiment, 1.4 versus 187.5 β-galactosidase-inducing units per ng of CA-p24 in a multinuclear activation of galactosidase indicator cell assay) (39). It well coincided with the data we got in the present study. As the inserted fragments of the four mutants were very similar in length and sequence (DDNLp4Δ1, 128 bases; DDNLp4Δ2, 144 bases; DDNLp4Δ3, 149 bases; and DDNLp4Δ4, 149 bases); a prominent replication defect of DDNLp4Δ2 might correlate with the appearance of monomeric genomes in virions, which is a unique feature of this mutant. Stepwise measurement of replication efficiency identified defects of the mutants in multiple steps of infection (Fig. 4C and D). Levels of viral DNA synthesis of DDNLp4Δ2 fell to around 15% of WT, whereas more than half of its viral DNA synthesis ability was retained in the DDNLp4Δ3 mutant. This difference strongly suggests a negative effect of the monomeric genome on reverse transcription. As the monomeric genome in virions of DDNLp4Δ2 accounted for 50% or less (Fig. 2B) of their content, the defect shown here occurred not only on the monomeric genome but also on the normal-looking dimeric genome of the mutants. These results seem to indicate that the inserted fragment of the mutant caused an abnormal secondary or tertiary structure of the overall viral RNA genome, resulting in poor reverse transcription. Viral genome dimerization and/or DIS was reported to play a role in efficient reverse transcription (6, 29), and our data supported these earlier arguments.

A multiround infection experiment clearly demonstrated significantly reduced growth kinetics of the mutants (Fig. 5). Moreover, inserted sequences of the mutants were completely deleted during the replication process, which strongly suggests that the insertion caused a fatal defect in viral replication. The appearance of revertants before the occurrence of compensation mutation implies that aberrant viral RNA conformation in these mutants was too drastic to be undone by protein modification.

In conclusion, in this study, we succeeded in identifying the essential region for HIV-1 genome dimer linkage formation in virions. Our consecutive experiments demonstrated that the dimerization region on RNA molecules may be important for the efficient progress of reverse transcription, probably by maintaining an appropriate form of viral genome in virions. A recent study has suggested that HIV-1 *pol* proteins contribute to genome RNA dimerization (8), which could be related to

our speculation. Further studies can be expected to provide more findings relevant to this hypothesis.

ACKNOWLEDGMENTS

This work was supported by grants from the Ministry of Education, Culture, Sports, Science and Technology; the Ministry of Health, Labor, and Welfare; and the Health Science Foundation of Japan.

REFERENCES

1. Abbink, T. E., and B. Berkhout. 2003. A novel long distance base-pairing interaction in human immunodeficiency virus type 1 RNA occludes the Gag start codon. *J. Biol. Chem.* 278:11601–11611.
2. Adachi, A., H. E. Gendelman, S. Koenig, T. Folks, R. Willey, A. Rabson, and M. A. Martin. 1986. Production of acquired immunodeficiency syndrome-associated retrovirus in human and nonhuman cells transfected with an infectious molecular clone. *J. Virol.* 59:284–291.
3. Aldovini, A., and B. D. Walker. 1990. *Techniques in HIV research*. Stockton Press, New York, NY.
4. Andersen, E. S., S. A. Contera, B. Knudsen, C. K. Damgaard, F. Besenbacher, and J. Kjems. 2004. Role of the trans-activation response element in dimerization of HIV-1 RNA. *J. Biol. Chem.* 279:22243–22249.
5. Beerens, N., F. Groot, and B. Berkhout. 2001. Initiation of HIV-1 reverse transcription is regulated by a primer activation signal. *J. Biol. Chem.* 276:31247–31256.
6. Berkhout, B., A. T. Das, and J. L. van Wamel. 1998. The native structure of the human immunodeficiency virus type 1 RNA genome is required for the first strand transfer of reverse transcription. *Virology* 249:211–218.
7. Brussel, A., and P. Sonigo. 2003. Analysis of early human immunodeficiency virus type 1 DNA synthesis by use of a new sensitive assay for quantifying integrated provirus. *J. Virol.* 77:10119–10124.
8. Buxton, P., G. Tachedjian, and J. Mak. 2005. Analysis of the contribution of reverse transcriptase and integrase proteins to retroviral RNA dimer conformation. *J. Virol.* 79:6338–6348.
9. Chin, M. P., T. D. Rhodes, J. Chen, W. Fu, and W. S. Hu. 2005. Identification of a major restriction in HIV-1 intersubtype recombination. *Proc. Natl. Acad. Sci. USA* 102:9002–9007.
10. Darlix, J. L., C. Gabus, and B. Allain. 1992. Analytical study of avian reticuloendotheliosis virus dimeric RNA generated in vivo and in vitro. *J. Virol.* 66:7245–7252.
11. Darlix, J. L., C. Gabus, M. T. Nugeyre, F. Clavel, and F. Barre-Sinoussi. 1990. *cis* elements and *trans*-acting factors involved in the RNA dimerization of the human immunodeficiency virus HIV-1. *J. Mol. Biol.* 216:689–699.
12. Götte, M., X. Li, and M. A. Wainberg. 1999. HIV-1 reverse transcription: a brief overview focused on structure-function relationships among molecules involved in initiation of the reaction. *Arch. Biochem. Biophys.* 365:199–210.
13. Graham, F. L., J. Smiley, W. C. Russell, and R. Nairn. 1977. Characteristics of a human cell line transformed by DNA from human adenovirus type 5. *J. Gen. Virol.* 36:59–74.
14. Höglund, S., Å. Öhagen, J. Goncalves, A. T. Panganiban, and D. Gabuzda. 1997. Ultrastructure of HIV-1 genomic RNA. *Virology* 233:271–279.
15. Hu, W. S., and H. M. Temin. 1990. Retroviral recombination and reverse transcription. *Science* 250:1227–1233.
16. Huthoff, H., and B. Berkhout. 2001. Mutations in the TAR hairpin affect the equilibrium between alternative conformations of the HIV-1 leader RNA. *Nucleic Acids Res.* 29:2594–2600.
17. Huthoff, H., and B. Berkhout. 2001. Two alternating structures of the HIV-1 leader RNA. *RNA* 7:143–157.
18. Ikeda, T., H. Nishitsuji, X. Zhou, N. Nara, T. Ohashi, M. Kannagi, and T. Masuda. 2004. Evaluation of the functional involvement of human immunodeficiency virus type 1 integrase in nuclear import of viral cDNA during acute infection. *J. Virol.* 78:11563–11573.
19. Julias, J. G., A. L. Ferris, P. L. Boyer, and S. H. Hughes. 2001. Replication of phenotypically mixed human immunodeficiency virus type 1 virions containing catalytically active and catalytically inactive reverse transcriptase. *J. Virol.* 75:6537–6546.
20. Koh, K. B., M. Fujita, and A. Adachi. 2000. Elimination of HIV-1 plasmid DNA from virus samples obtained from transfection by calcium-phosphate co-precipitation. *J. Virol. Methods* 90:99–102.
21. Marquet, R., F. Baudin, C. Gabus, J. L. Darlix, M. Mougé, C. Ehresmann, and B. Ehresmann. 1991. Dimerization of human immunodeficiency virus (type 1) RNA: stimulation by cations and possible mechanism. *Nucleic Acids Res.* 19:2349–2357.
22. Marquet, R., J. C. Paillart, E. Skripkin, C. Ehresmann, and B. Ehresmann. 1994. Dimerization of human immunodeficiency virus type 1 RNA involves sequences located upstream of the splice donor site. *Nucleic Acids Res.* 22:145–151.
23. McBride, M. S., and A. T. Panganiban. 1996. The human immunodeficiency virus type 1 encapsidation site is a multipartite RNA element composed of functional hairpin structures. *J. Virol.* 70:2963–2973.

24. McBride, M. S., and A. T. Panganiban. 1997. Position dependence of functional hairpins important for human immunodeficiency virus type 1 RNA encapsidation in vivo. *J. Virol.* 71:2050–2058.
25. McBride, M. S., M. D. Schwartz, and A. T. Panganiban. 1997. Efficient encapsidation of human immunodeficiency virus type 1 vectors and further characterization of *cis* elements required for encapsidation. *J. Virol.* 71:4544–4554.
26. Moumen, A., L. Polomack, B. Roques, H. Buc, and M. Negroni. 2001. The HIV-1 repeated sequence R as a robust hot-spot for copy-choice recombination. *Nucleic Acids Res.* 29:3814–3821.
27. Nagao, T., A. Yoshida, A. Sakurai, A. Piroozmand, A. Jere, M. Fujita, T. Uchiyama, and A. Adachi. 2004. Determination of HIV-1 infectivity by lymphocytic cell lines with integrated luciferase gene. *Int. J. Mol. Med.* 14:1073–1076.
28. Ohishi, M., T. Shioda, and J. I. Sakuragi. 2007. Retro-transduction by virus pseudotyped with glycoprotein of vesicular stomatitis virus. *Virology* 362:131–138.
29. Paillart, J. C., L. Berthou, M. Ottmann, J. L. Darlix, R. Marquet, B. Ehresmann, and C. Ehresmann. 1996. A dual role of the putative RNA dimerization initiation site of human immunodeficiency virus type 1 in genomic RNA packaging and proviral DNA synthesis. *J. Virol.* 70:8348–8354.
30. Paillart, J. C., R. Marquet, E. Skripkin, C. Ehresmann, and B. Ehresmann. 1996. Dimerization of retroviral genomic RNAs: structural and functional implications. *Biochimie* 78:639–653.
31. Paillart, J. C., M. Shehu-Xhilaga, R. Marquet, and J. Mak. 2004. Dimerization of retroviral RNA genomes: an inseparable pair. *Nat. Rev. Microbiol.* 2:461–472.
32. Paillart, J. C., E. Skripkin, B. Ehresmann, C. Ehresmann, and R. Marquet. 2002. In vitro evidence for a long range pseudoknot in the 5'-untranslated and matrix coding regions of HIV-1 genomic RNA. *J. Biol. Chem.* 277:5995–6004.
33. Paillart, J. C., E. Skripkin, B. Ehresmann, C. Ehresmann, and R. Marquet. 1996. A loop-loop "kissing" complex is the essential part of the dimer linkage of genomic HIV-1 RNA. *Proc. Natl. Acad. Sci. USA* 93:5572–5577.
34. Prats, A. C., C. Roy, P. A. Wang, M. Erard, V. Housset, C. Gabus, C. Paoletti, and J. L. Darlix. 1990. *cis* elements and *trans*-acting factors involved in dimer formation of murine leukemia virus RNA. *J. Virol.* 64:774–783.
35. Rein, A. 2004. Take two. *Nat. Struct. Mol. Biol.* 11:1034–1035.
36. Roy, C., N. Tounekti, M. Mougel, J. L. Darlix, C. Paoletti, C. Ehresmann, B. Ehresmann, and J. Paoletti. 1990. An analytical study of the dimerization of in vitro generated RNA of Moloney murine leukemia virus MoMuLV. *Nucleic Acids Res.* 18:7287–7292.
37. Russell, R. S., C. Liang, and M. A. Wainberg. 2004. Is HIV-1 RNA dimerization a prerequisite for packaging? Yes, no, probably? *Retrovirology* 1:23.
38. Russell, R. S., A. Roldan, M. Detorio, J. Hu, M. A. Wainberg, and C. Liang. 2003. Effects of a single amino acid substitution within the p2 region of human immunodeficiency virus type 1 on packaging of spliced viral RNA. *J. Virol.* 77:12986–12995.
39. Sakuragi, J., A. Iwamoto, and T. Shioda. 2002. Dissociation of genome dimerization from packaging functions and virion maturation of human immunodeficiency virus type 1. *J. Virol.* 76:959–967.
40. Sakuragi, J., T. Shioda, and A. T. Panganiban. 2001. Duplication of the primary encapsidation and dimer linkage region of HIV-1 RNA results in the appearance of monomeric RNA in virions. *J. Virol.* 75:2557–2565.
41. Sakuragi, J., S. Ueda, A. Iwamoto, and T. Shioda. 2003. Possible role of dimerization in human immunodeficiency virus type 1 genome RNA packaging. *J. Virol.* 77:4060–4069.
42. Sakuragi, J. I., and A. T. Panganiban. 1997. Human immunodeficiency virus type 1 RNA outside the primary encapsidation and dimer linkage region affects RNA dimer stability in vivo. *J. Virol.* 71:3250–3254.
43. Willey, R. L., D. H. Smith, L. A. Lasky, T. S. Theodore, P. L. Earl, B. Moss, D. J. Capon, and M. A. Martin. 1988. In vitro mutagenesis identifies a region within the envelope gene of the human immunodeficiency virus that is critical for infectivity. *J. Virol.* 62:139–147.
44. Zuker, M. 1989. On finding all suboptimal foldings of an RNA molecule. *Science* 244:48–52.

Potent Inhibition of HIV-1 Replication by Novel Non-peptidyl Small Molecule Inhibitors of Protease Dimerization*

Received for publication, May 14, 2007, and in revised form, June 25, 2007. Published, JBC Papers in Press, July 17, 2007, DOI 10.1074/jbc.M703938200

Yasuhiro Koh^{‡§}, Shintaro Matsumi^{‡§}, Debananda Das[¶], Masayuki Amano^{‡§}, David A. Davis^{||}, Jianfeng Li^{**}, Sofiya Leschenko^{**}, Abigail Baldrige^{**}, Tatsuo Shioda^{**}, Robert Yarchoan^{||}, Arun K. Ghosh^{**}, and Hiroaki Mitsuya^{‡§¶1}

From the [‡]Department of Hematology and [§]Department of Infectious Diseases, Kumamoto University Graduate School of Medical and Pharmaceutical Sciences, 1-1-1 Honjo, Kumamoto 860-8556, Japan, the [¶]Experimental Retrovirology Section and ^{||}Retroviral Disease Section, HIV and AIDS Malignancy Branch, NCI, National Institutes of Health, Bethesda, Maryland 20892, the ^{**}Departments of Chemistry and Medicinal Chemistry, Purdue University, West Lafayette, Indiana 47907, and the ^{**}Department of Viral Infections, Research Institute for Microbial Diseases, Osaka University, Osaka 565-0871, Japan

Dimerization of HIV-1 protease subunits is essential for its proteolytic activity, which plays a critical role in HIV-1 replication. Hence, the inhibition of protease dimerization represents a unique target for potential intervention of HIV-1. We developed an intermolecular fluorescence resonance energy transfer-based HIV-1-expression assay employing cyan and yellow fluorescent protein-tagged protease monomers. Using this assay, we identified non-peptidyl small molecule inhibitors of protease dimerization. These inhibitors, including darunavir and two experimental protease inhibitors, blocked protease dimerization at concentrations of as low as 0.01 μM and blocked HIV-1 replication with IC_{50} values of 0.0002–0.48 μM . These agents also inhibited the proteolytic activity of mature protease. Other approved anti-HIV-1 agents examined except tipranavir, a CCR5 inhibitor, and soluble CD4 failed to block the dimerization event. Once protease monomers dimerize to become mature protease, mature protease is not dissociated by this dimerization inhibition mechanism, suggesting that these agents block dimerization at the nascent stage of protease maturation. The proteolytic activity of mature protease that managed to undergo dimerization despite the presence of these agents is likely to be inhibited by the same agents acting as conventional protease inhibitors. Such a dual inhibition mechanism should lead to highly potent inhibition of HIV-1.

ever, eradication of human immunodeficiency virus, type 1 (HIV-1)² does not appear to be currently possible, in part due to the viral reservoirs remaining in blood and infected tissues. Moreover, a number of challenges have been encountered, which include various adverse effects, only partial and limited immunologic restorations achieved, and occurrence of various cancers as consequences of survival elongation with highly active antiretroviral therapy (1). Moreover, such limitations of highly active antiretroviral therapy are exacerbated by the development of drug-resistant HIV-1 variants (2). Thus, the identification of new classes of antiretroviral drugs that have one or more unique mechanisms of action and produce no or minimal adverse effects remains an important therapeutic objective.

Dimerization of HIV-1 protease subunits is an essential process for the acquisition of proteolytic activity of HIV-1 protease, which plays a critical role in the maturation and replication of the virus (3, 4). Thus inhibition of protease dimerization by chemical reagents is likely to abolish proteolytic activity and inhibit HIV-1 replication. However, for possible development of HIV-1 protease dimerization inhibitors, better understanding of the nature and dynamics of protease dimerization is crucial. The monomer subunits are connected by polar and non-polar interactions to form the dimer. Hydrophobicity of Leu-89, Leu-90, and Ile-93 and several other residues have been considered important in the folding of a protease monomer as well as in dimer stabilization (5, 6). For a systematic analysis of the conserved network of hydrogen bonds, termed “fireman’s grip,” Strisovsky *et al.* (7) have mutated the active site Thr-26 to a Ser, Cys, or Ala and have shown that T26A substitution reduced protease dimer stability, thus virtually nullifying the proteolytic activity of protease. Indeed, in our present study, T26A substitution effectively disrupted protease dimerization (see below), corroborating the results by Strisovsky *et al.* The flexibility of monomeric and dimeric HIV-1 protease and the feasibility of a stable protease monomer have also been studied

Highly active antiretroviral therapy has had a major impact on the AIDS epidemic in industrially advanced nations. How-

* This work was supported by the Intramural Research Program of Center for Cancer Research, NCI, National Institutes of Health (NIH), by a Grant-in-aid for Scientific Research (Priority Areas) from the Ministry of Education, Culture, Sports, Science, and Technology of Japan (Monbu-Kagakusho), a Grant for Promotion of AIDS Research from the Ministry of Health, Welfare, and Labor of Japan (Kosei-Rohdoshu), by the Cooperative Research Project on Clinical and Epidemiological Studies of Emerging and Re-emerging Infectious Diseases (Renkei Jigyo: Grant 78, Kumamoto University) of Monbu-Kagakusho, by the Japan Health Sciences Foundation (International Research Grant SA14801 to H. M. and A. K. G.), and by NIH Grant GM 53386 (to A. K. G.). The costs of publication of this article were defrayed in part by the payment of page charges. This article must therefore be hereby marked “advertisement” in accordance with 18 U.S.C. Section 1734 solely to indicate this fact.

¹ To whom correspondence should be addressed: Tel.: 81-96-373-5156; Fax: 81-96-363-5265; E-mail: hmitsuya@helix.nih.gov.

² The abbreviations used are: HIV-1, human immunodeficiency virus, type 1; FRET, fluorescence resonance energy transfer; CFP, cyan fluorescent protein; YFP, yellow fluorescent protein; BCV, brecaonavir; DRV, darunavir; CHX, cycloheximide; PI, protease inhibitor; bis-THF, bistetrahydrofuranylurethane; TPV, tipranavir; Fluc, firefly luminescence; Rluc, *Renilla* luminescence; RT, reverse transcriptase; PR, protease.

Potent HIV-1 Inhibition and Protease Dimerization Inhibition

by computational simulation (8, 9). There are four anti-parallel β -sheets involving the N and C termini of both monomer subunits and they contribute close to 75% of the dimerization energy (10), explaining at least in part why DRV failed to dissociate mature protease dimer (see below). The termini interface has been explored as a dimerization inhibition target by several groups (11–13). We have also recently reported that certain peptides containing the dimer interface sequences amino acids 1–5 and amino acids 95–99 blocked HIV-1 infectivity and replication (14). However, to the best of our knowledge, no evidence of direct dimerization inhibition by such compounds has been yet documented.

In the present study, we developed an intermolecular fluorescence resonance energy transfer (FRET)-based HIV-1-expression assay that employed cyan and yellow fluorescent protein-tagged HIV-1 protease monomers. Using this assay, we identified a group of non-peptidyl small molecule inhibitors of HIV-1 protease dimerization. These inhibitors, including the recently approved protease inhibitor (PI) darunavir (DRV) as well as two experimental protease inhibitors (PIs), blocked protease dimerization at concentrations of as low as 0.01 μM and blocked HIV-1 replication *in vitro* with IC_{50} values of 0.0002–0.48 μM . These agents also inhibited the proteolytic activity of mature HIV-1 protease. Another PI, tipranavir (TPV), active against HIV-1 variants resistant to multiple PIs, also blocked protease dimerization, although all other existing FDA-approved anti-HIV-1 drugs examined in the present study failed to block the dimerization. The present report represents the first demonstration that non-peptidic small molecule agents can disrupt protease dimerization.

EXPERIMENTAL PROCEDURES

Generation of FRET-based HIV-1 Expression System—Cyan fluorescent protein (CFP)- and yellow fluorescent protein (YFP)-tagged HIV-1 protease constructs were generated using BD Creator™ DNA cloning kits (BD Biosciences, San Jose, CA). First, XhoI/HindIII fragments from pCR-XL-TOPO vector containing the HIV-1 protease-encoding gene excised from pHIV-1_{NL4-3} was inserted into the pDNR-1r (donor vector) that had been digested with XhoI and HindIII. In the transfer of the protease gene from the donor vector into pLP-CFP/YFP-C1 (acceptor vector), the Cre-loxP site-specific recombination method was used according to manufacturer's instructions. Using Cre-recombinase with the lox P site, the protease gene from pDNR-1r was inserted into pLP-CFP-C1 or pLP-YFP-C1 through Cre-mediated recombination (15), generating a plasmid of CFP-tagged wild type protease (PR_{WT}) and that of YFP-tagged PR_{WT}, with which HIV-1 protease was successfully expressed as a fusion protein with CFP- and YFP-tagged at the C terminus, respectively. Western blot assay using anti-green fluorescent protein-specific rabbit polyclonal antibodies revealed that protease was correctly tagged to CFP or YFP (data not shown).

For the generation of full-length molecular infectious clones containing CFP- or YFP-tagged protease, the PCR-mediated recombination method was used (16). To this end, we amplified an upstream proviral DNA fragment containing ApaI site and HIV-1 protease (excised from pHIV-1_{NL4-3}) with a primer pair: Apa-PRO-F (5'-TTG CAG GGC CCC TAG GAA AAA GG-3')

plus PR-5Ala-R (5'-GGC TGC TGC GGC AGC AAA ATT TAA AGT GCA GCC AAT CT-3'), a middle proviral DNA fragment containing CFP (excised from pCFP-C1) or YFP (excised from pYFP-C1) (Clontech, Mountain View, CA) with a primer pair: CFPYFP-5Ala-F (5'-GCT GCC GCA GCA GCC GTG AGC AAG GGC GAG GAG CTG-3') plus CFPYFP-FP-R (5'-ACT AAT GGG AAA CTT GTA CAG CTC GTC CAT GCC G-3'), and a downstream proviral DNA fragment containing the 5'-DNA fragment of reverse transcriptase (RT) and SmaI site from pHIV-1_{NLS_{Sma}} (17), which had been created to have a SmaI site by changing two nucleotides (2590 and 2593) of pHIV-1_{NL4-3} with a primer pair: FRT-F (5'-TTT CCC ATT AGT CCT ATT GAG ACT GTA-3') plus NL4-3-RT263-R (5'-CCA GAA ATC TTG AGT TCT CTT ATT-3'). A linker consisting of five alanines was inserted between protease and fluorescent protein. The phenylalanine-proline site that HIV-1 protease cleaves was also introduced between the fluorescent protein and RT. Thus obtained three DNA fragments were subsequently joined by using the PMR reaction performed under the standard condition for ExTaq polymerase (Takara Bio Inc., Otsu, Japan) with 10 pmol of Apa-PRO-F (5'-TTG CAG GGC CCC TAG GAA AAA GG-3') and NL4-3-RT263-R (5'-CCA GAA ATC TTG AGT TCT CTT ATT-3') and the three DNA fragments (100 ng each) in a 20- μl reaction solution. Thermal cycling was carried out as follows: 94 °C for 3 min, followed by 35 cycles of 94 °C for 50 s, 53 °C for 50 s, and 72 °C for 2 min, and finally by 72 °C for 15 min. The amplified PCR products were cloned into pCR-XL-TOPO vector according to the manufacturer's instructions (Gateway Cloning System, Invitrogen). PCR products were generated with pCR-XL-TOPO vector as templates, followed by digestion by both ApaI and SmaI, and the ApaI-SmaI fragment was introduced into pHIV-1_{NLS_{Sma}} (17), generating pHIV-PR_{WT}^{CFP} and pHIV-PR_{WT}^{YFP}, respectively.

Analysis of Inter- and Intra-molecule Interactions of Protease Subunits—Analysis of inter- and intra-molecule interactions of protease subunits was conducted by employing the crystal structure of DRV with HIV-1 protease (PDB ID: 2IEN). Hydrogens were added and minimized using the OPLS2005 force field with constraints on heavy atom positions. The calculation was performed using MacroModel 9.1 from Schrödinger, LLC. Hydrogen bonds were assigned when the following distance and angle cut-off was satisfied: 3.0 Å for H-A distance; D-H-A angle >90°; and H-A-B angle >60° where H is the hydrogen, A is the acceptor, D is the donor, and B is a neighbor atom bonded to the acceptor. The representative distance between the termini of two monomers was determined by analyzing the protease-DRV crystal structure (PDB ID: 2IEN). The distance between the α carbons at the N termini and C termini is around 0.5 nm, whereas the distance between the α carbons of the N termini ends of two monomers is around 1.8 nm.

FRET Procedure—COS7 cells plated on EZ view cover-glass bottom culture plate (Iwaki, Tokyo) were transfected with the indicated plasmid constructs using Lipofectamine 2000 (Invitrogen) according to manufacturer's instructions in the presence of various concentrations of each compound, cultured for 72 h, and analyzed under Fluoview FV500 confocal laser scanning microscope (Olympus Optical Corp., Tokyo) at room

temperature. When the effect of each compound was analyzed by FRET, test compounds were added to the culture medium simultaneously with plasmid transfection.

The results of FRET were determined by quenching of CFP (donor) fluorescence and an increase in YFP (acceptor) fluorescence (sensitized emission), because part of the energy of CFP is transferred to YFP instead of being emitted. This phenomenon can be measured by bleaching YFP, which should result in an increase in CFP fluorescence. This technique, also known as acceptor photobleaching, is a well established method of determining the occurrence of FRET (18–21). Dequenching of the donor CFP by selective photobleaching of the acceptor YFP was performed by first obtaining YFP and CFP images at the same focal plane, followed by illuminating for 3 min the same image at a wavelength of 488 nm with a laser power set at the maximum intensity to bleach YFP and re-capturing the same CFP and YFP images. The changes in the CFP and YFP fluorescence intensity in the images of selected regions were examined and quantified using Olympus FV500 Image software system (Olympus Optical Corp.). Background values were obtained from the regions where no cells were present and were subtracted from the values for the cells examined in all calculations. For each chimeric protein, the data were obtained from at least three independent experiments. Digitized image data obtained from the experiment were prepared for presentation using Photoshop 6.0 (Adobe Systems, Mountain View, CA). Ratios of intensities of CFP fluorescence after photobleaching to CFP fluorescence prior to photobleaching (CFP^{A/B} ratios) were determined. It is well established that the CFP^{A/B} ratios of >1.0 indicate that association of CFP- and YFP-tagged proteins occurred, and it was interpreted that the dimerization of protease subunits occurred. When the CFP^{A/B} ratios were <1, it indicated that the association of the two subunits did not occur, and it was interpreted that protease dimerization was inhibited.

Non-peptidyl Small Molecule Compounds—Seven non-peptidyl small molecule compounds were synthesized in a convergent manner by coupling an optically active P2 ligand and an (*R*)-hydroxyethylamino sulfonamide isostere (22). Synthetic methods for TMC126 and DRV have been previously described (22, 23). Detailed synthetic methods for the other four compounds will be described elsewhere. TPV was obtained through the AIDS Research and Reference Reagent Program, Division of AIDS, NIAID, National Institutes of Health.

Dual Luciferase Assay—Dual luciferase assay was established using the CheckMate™ Mammalian Two-Hybrid System (Promega Corp., Madison, WI). Briefly, BamHI/KpnI fragments from pCR-XL-TOPO vector containing the HIV-1 protease (PR_{WT})-encoding gene excised from pHIV-1_{NL4-3} was inserted into the pACT vector and pBIND vector that had been digested with BamHI and KpnI, generating pACT-PR_{wt} and pBIND-PR_{wt}, which produced an in-frame fusion of wild-type HIV-1 protease downstream of the VP16 activation domain and GAL4 DNA-binding domain, respectively. COS7 cells were co-transfected with pACT-PR_{wt}, pBIND-PR_{wt}, and pG5luc in the absence or presence of 0.1 or 1.0 μM DRV in white 96-well flat bottom plates (Corning, NY), cultured for 48 h, and the

intensity of firefly luminescence (Fluc) and *Renilla* luminescence (Rluc) was measured with TR717 microplate luminometer (Applied Biosystems) according to the manufacturer's instructions. DRV was added to the culture medium simultaneously with plasmids to be used. Fluc/Rluc intensity ratios were determined with co-transfection of pACT-PR_{WT}, pBIND-PR_{WT}, and pG5luc in the absence of DRV, serving as maximal values. Fluc/Rluc intensity ratios determined with co-transfection of a pACT vector, a pBIND vector, and pG5luc served as minimal (background) values. Relative response ratios (RRR) were determined using the following formula: $RRR = [(experimental\ Fluc/Rluc) - (negative\ control\ Fluc/Rluc)] / [(positive\ control\ Fluc/Rluc) - (negative\ control\ Fluc/Rluc)]$.

Drug Susceptibility Assay—The susceptibility of HIV-1_{LAI} to various drugs and their cytotoxicity were determined using the 3-(4,5-dimethylthiazol-2-yl)-2,5-diphenyltetrazolium bromide assay as previously described (24). Briefly, MT-2 cells (2 × 10⁴/ml) were exposed to 100 50% tissue culture infectious doses (TCID₅₀s) of HIV-1_{LAI} in the presence or absence of various concentrations of drugs in 96-well microculture plates and cultured at 37 °C for 7 days. After 100 μl of the medium was removed from each well, 3-(4,5-dimethylthiazol-2-yl)-2,5-diphenyltetrazolium bromide solution (10 μl, 7.5 mg/ml in phosphate-buffered saline) was added to each well, followed by incubation at 37 °C for 4 h. After incubation, 100 μl of acidified isopropanol containing 4% (v/v) Triton X-100 was added to each well, to dissolve the formazan crystals, and the optical density was measured in a kinetic microplate reader (*V*_{max}, Molecular Devices, Sunnyvale, CA). All assays were performed in duplicate or triplicate. In some experiments, MT-2 cells were chosen as target cells in the 3-(4,5-dimethylthiazol-2-yl)-2,5-diphenyltetrazolium bromide assay, because these cells undergo greater HIV-1-elicited cytopathic effects than MT-4 cells.

Enzyme Kinetics—The chromogenic substrate Lys-Ala-Arg-Val-Nle-paranitro-Phe-Glu-Ala-Nle-amide (Sigma) was used to determine the kinetic parameters (25, 26). Wild-type protease, at final concentrations of 160–190 nM, was added to varying concentrations of substrate (100–400 μM) maintained in 50 mM sodium acetate (pH 5.0), 0.1 M NaCl, 1 mM EDTA, and assayed by monitoring the decrease in absorbance at 310 nm using a Varian Cary 100Bio UV-visible spectrophotometer. The *k*_{cat} and *K*_m values were obtained employing standard data fitting techniques for a reaction obeying Michaelis-Menten kinetics. The data curves were fitted using SigmaPlot 8.0.2 (SPSS Inc., Chicago, IL). The active enzyme concentrations were calculated from the intercept of the linear fit to the IC₅₀ versus [S] plots with the IC₅₀ axis. The *K*_i values were obtained from the IC₅₀ values estimated from an inhibitor dose-response curve with the spectroscopic assay using the equation $K_i = (IC_{50} - [E]/2) / (1 + [S]/K_m)$, where [E] and [S] are the protease and substrate concentrations, respectively (27). The *K*_i values were measured at four to five substrate concentrations. The measurement was repeated at least three times to produce the average values.

Assay for Effects of Darunavir on Dimerized Mature Protease—To examine whether a representative dimerization inhibitor, DRV, could dissociate mature protease that had already been

Potent HIV-1 Inhibition and Protease Dimerization Inhibition

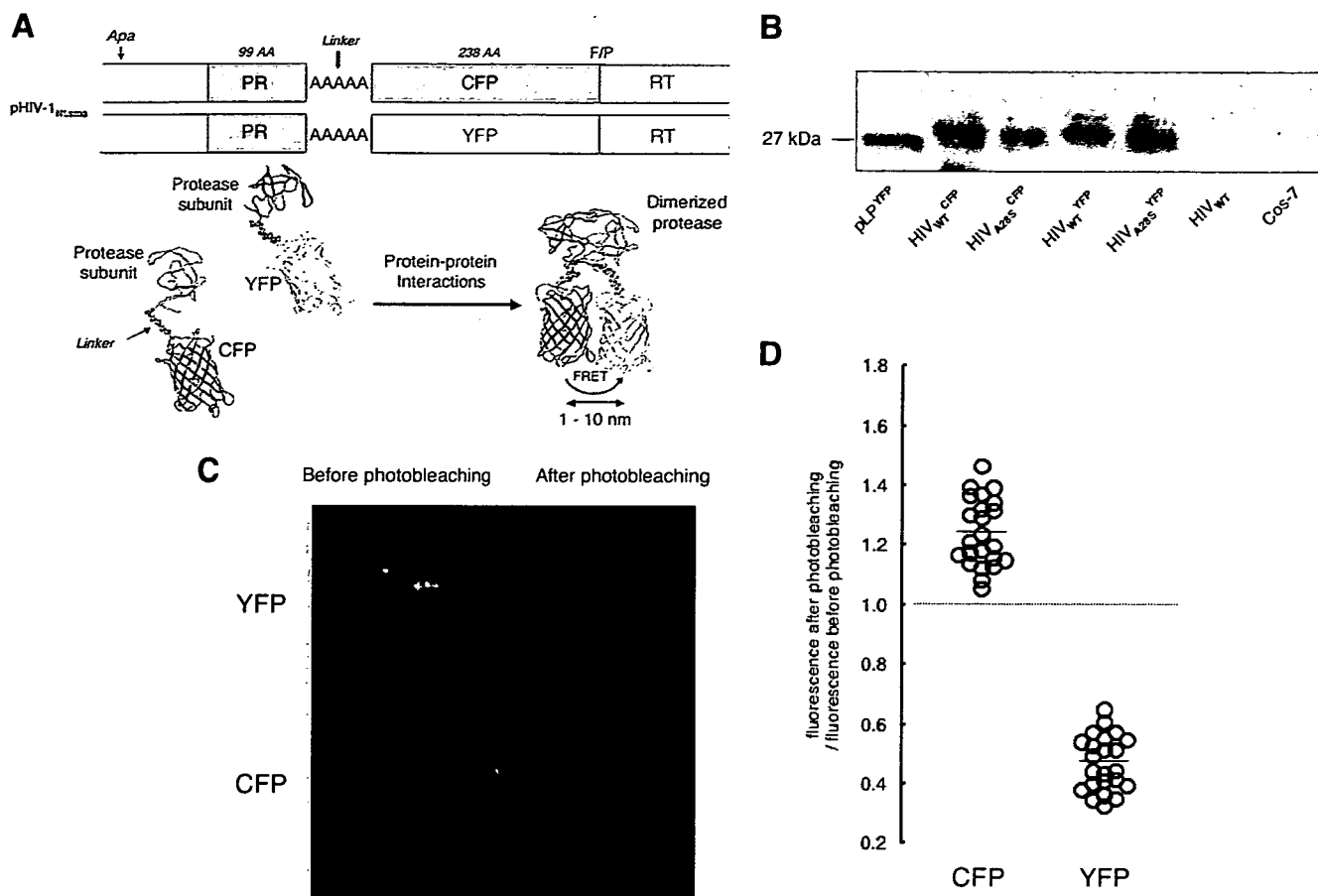


FIGURE 1. FRET-based HIV-1 expression system. *A*, generation of FRET-based HIV-1 expression system. Various plasmids encoding full-length molecular infectious HIV-1 (HIV-1_{NL4-3}) clones producing CFP- or YFP-tagged protease using the PCR-mediated recombination method were prepared. A linker consisting of five alanines was introduced between protease and fluorescent protein. A phenylalanine-proline site (F/P) that HIV-1 protease cleaves was also introduced between the fluorescent protein and RT. Shown are structural representations of protease monomers and dimer in association with the linker atoms and fluorescent proteins. FRET occurs only when the fluorescent proteins are 1–10 nm apart. *B*, expression of CFP- and YFP-tagged wild-type HIV-1 protease. To confirm the presence of HIV-1 protease tagged to fluorescent protein in COS7 cells transfected with a plasmid encoding HIV_{wt}-CFP, HIV_{A285}-CFP, HIV_{wt}-YFP, or HIV_{A285}-YFP, Western blot analysis was performed using lysates of pelleted virions. The CFP- and YFP-tagged proteases were visualized by SuperSignal WestPico Chemiluminescent Substrates using polyclonal anti-GFP antiserum and ECL anti-rabbit IgG peroxidase-linked species-specific whole antibody. pLP^{YFP} denotes the lysates of cells transfected with a plasmid encoding only YFP. The lysates of COS7 cells transfected with a plasmid encoding HIV_{wt}, and those of untreated COS7 cells serve as controls. *C*, fluorescence images of co-transfected cells prior to and after acceptor photobleaching. COS7 cells plated on EZ view cover-glass bottom culture plate were transfected with two plasmids, pPR_{wt}-CFP and pPR_{wt}-YFP, using Lipofectamine, cultured for 72 h, and analyzed under a Fluoview FV500 confocal laser scanning microscope. Both PR_{wt}-CFP and PR_{wt}-YFP proteins were visualized prior to photobleaching. Note that photobleaching of the cells dramatically reduced YFP fluorescence with a YFP^{A/B} ratio of 0.17 and increased CFP emission with a CFP^{A/B} ratio of 1.38, signifying the dimerization of both YFP- and CFP-tagged protease subunits. *D*, ratios of the emission intensities before and after photobleaching. Fluorescence intensities of each cell transfected with two plasmids, pPR_{wt}-CFP and pPR_{wt}-YFP, were measured before and after photobleaching, and ratios of the emission intensities before and after photobleaching (CFP^{A/B} ratios) were determined, and plotted. The CFP^{A/B} ratio values were 1.24 ± 0.11 ($n = 23$), whereas the YFP^{A/B} ratio values were 0.47 ± 0.09 ($n = 23$). The mean of these ratios are shown as bars.

dimerized, COS7 cells were co-transfected with a pair of plasmids encoding HIV-PR_{wt}-CFP and HIV-PR_{wt}-YFP and exposed to a protein synthesis inhibitor cycloheximide (CHX, 50 μ g/ml, Sigma) at 24, 48, 72, and 96 h of culture following transfection. The cells were then exposed to DRV (1 μ M) on day 5 of culture, and the values of the CFP^{A/B} ratio were determined at various time points. When the CFP^{A/B} ratios determined were >1.0 , it was determined that HIV-1 protease had been generated and dimerization had occurred. The production of HIV-1 was monitored every 24 h following transfection by determining levels of p24 Gag protein produced into culture medium as previously described (24).

RESULTS

Generation of FRET-based HIV-1 Expression Assay—The basic concepts of the intermolecular FRET-based HIV-1-ex-

pression assay (FRET-HIV-1 assay) are shown in Fig. 1. Within a plasmid (pHIV-1_{NL4-3}), which encodes a full-length molecular infectious HIV-1 clone, the gene encoding a CFP was attached to the downstream end (C terminus) of the gene encoding an HIV-1 protease subunit through the flexible linker added (five alanines), generating pHIV-1_{NL4-3}/CFP (Fig. 1A). Within the other plasmid (pHIV-1_{NL4-3}), the gene encoding a YFP was attached to the downstream end of protease-encoding gene in the same manner, generating pHIV-1_{NL4-3}/YFP. Both CFP and YFP were designed to have phenylalanine and proline in the connection with RT so that the protease is cleaved from RT when two subunits dimerize and the dimerized protease acquires enzymatic activity. Fig. 1B illustrates that HIV-1 virions generated in COS7 cells transfected with pHIV-1_{NL4-3}/CFP contained CFP-tagged protease and those in COS7 cells transfected with pHIV-1_{NL4-3}/YFP contained YFP-tagged protease as

examined in Western blotting. The HIV-1 virions produced were capable of infecting CD4⁺ MT-4 cells when the cells were exposed to the supernatant of the transfected COS7 cells (data not shown), indicating that the expressed tagged protease was enzymatically and virologically functional. In the cytoplasm of COS7 cells co-transfected with pHIV-1_{NL4-3}/CFP and pHIV-1_{NL4-3}/YFP, a CFP-tagged protease subunit interacts and dimerizes with a YFP-tagged protease subunit, and CFP and YFP get close because the termini are separated by only 0.5 to 1.8 nm in the dimeric form of protease (note: the representative distance was determined by analyzing the protease-DRV crystal structure (PDB ID: 2IEN)). A focused laser beam excitation of CFP (triggered by helium-cadmium laser) results in rapid energy transfer to YFP, and most of the fluorescence photons are emitted by YFP (28). If the dimerization is blocked, the average distance between CFP and YFP become larger, the energy transfer rate is decreased, and the fraction of photons emitted by YFP is lowered.

To help us interpret the energy transfer efficiency quantitatively, we used the acceptor photobleaching technique, in which the change in CFP emission quenching is measured by comparing the value before and after selectively photobleaching YFP, which prevents problems associated with variable expression levels. In this acceptor photobleaching approach, when FRET occurs, the fluorescence of the CFP donor increases after bleaching the YFP acceptor chromophore, which is recognized as a signature for FRET (18). Thus, the analysis of the change in CFP fluorescence intensity in the same specimen regions, before and after removal of the acceptor, directly relates the energy transfer efficiency to both donor and acceptor fluorescence. Fig. 1C illustrates representative images of co-transfected cells prior to and after YFP photobleaching, showing that, following photobleaching, YFP fluorescence of YFP-tagged wild-type protease subunit (PR_{WT}^{YFP}) was decreased, whereas CFP fluorescence of PR_{WT}^{CFP} increased.

To further help us evaluate the energy transfer efficiency, we determined the ratios of cyan fluorescence intensity, determined with a confocal laser scanning microscope, after photobleaching over that before photobleaching (hereafter referred to as CFP^{A/B} ratios). We also determined YFP^{A/B} ratios in the same manner. If the CFP^{A/B} ratios are >1.0, it is thought the energy transfer (or FRET) took place (18), signifying that dimerization of PR_{WT}^{CFP} and PR_{WT}^{YFP} subunits occurred. Fig. 1D shows that in the co-transfected COS7 cells ($n = 23$), the CFP^{A/B} ratios were all >1.0 (CFP^{A/B} ratios, 1.24 ± 0.11 ; YFP^{A/B} ratios, 0.47 ± 0.09), demonstrating that dimerization of protease subunits occurred.

Changes in Fluorescence Emission with Amino Acid Substitutions in Protease—First, it was determined whether the above-described FRET-HIV-1 assay could be used to detect the disruption of HIV-1 protease dimerization. Five amino acids at the N terminus and those at the C terminus have been shown to be critical for protease dimerization (29). As shown in Fig. 2A, two protease monomer subunits are connected by four antiparallel β -sheets involving the N and C termini of both subunits. It is of note that mature dimerized protease has as many as 12 hydrogen bonds in this N- and C-terminal region. Thus, we introduced a Pro-1 to Ala substitution (P1A), Q2A, I3A, T4A, L5A,

T96A, L97A, N98A, or F99A substitution into the replication-competent HIV-1_{NL4-3} and found that I3A, L5A, T96A, L97A, and F99A disrupted protease dimerization, although other substitutions did not disrupt the dimerization.

Several amino acid substitutions outside the N and C termini have also been known to play a role in HIV-1 protease dimerization. Ishima and Louis and their colleagues have demonstrated that the introduction of T26A, D29N, D29A, or R87K to HIV-1 protease disrupts the dimer interface contacts and destabilizes protease dimer, causing the inhibition of protease dimerization (30–32). Fig. 2 (B and C) shows the locations of intermolecular hydrogen bonds formed by such amino acids between two monomer subunits. The hydrogen bond interactions between two subunits occur between Asp-29 and Arg-8', Arg-87 and Leu-5', Leu-24 and Thr-26', and Thr-26 and Thr-26'. There are also intra-molecular hydrogen bond interactions between Asp-29 and Arg-87 as shown in Fig. 2 (B–D). Thus, mutations in those amino acids were introduced into HIV-PR_{WT}^{CFP} and HIV-PR_{WT}^{YFP}, generating HIV-PR_{T26A}^{CFP}, HIV-PR_{T26A}^{YFP}, HIV-PR_{D29N}^{CFP}, HIV-PR_{D29N}^{YFP}, HIV-PR_{D29A}^{CFP}, HIV-PR_{D29A}^{YFP}, HIV-PR_{R87K}^{CFP}, and HIV-PR_{R87K}^{YFP}. Co-transfection of COS7 cells with a pair of CFP- and YFP-tagged protease-carrying HIV-1-encoding plasmids demonstrated that these four amino acid substitutions disrupted protease dimerization (the average CFP^{A/B} ratios were all <1.0; Fig. 2E). Substitutions of two amino acids adjacent to Asp-29 were also introduced, generating HIV-PR_{A28S}^{CFP}, HIV-PR_{A28S}^{YFP}, HIV-PR_{D30N}^{CFP}, and HIV-PR_{D30N}^{YFP}. Both A28S and D30N are known primary amino acid substitutions, conferring resistance to TMC126 and nelfinavir on HIV-1, respectively (33, 34). The fact that A28S- or D30N-containing HIV-1 is infectious and replication-competent indicates that these two amino acid substitutions would not disrupt protease dimerization. HIV-1 virions generated in COS7 cells transfected with HIV-PR_{A28S}^{CFP} and HIV-PR_{A28S}^{YFP} were confirmed to contain CFP-tagged protease and YFP-tagged protease in Western blotting, respectively (Fig. 1B). As expected, neither substitution disrupted the dimerization as examined in the FRET-HIV-1 assay (Fig. 2E). Another mutation D25A, which is adjacent to Thr²⁶ and is known to abrogate replicative activity of HIV-1 (35), failed to disrupt protease dimerization, indicating that the inability of D25A mutation-carrying HIV-1 to replicate is not due to dimerization disruption, but due to the loss of proteolytic activity of dimerized HIV-1 protease. Analysis of these data indicated that the FRET-HIV-1 assay system is a reliable tool to evaluate agents for their potential to inhibit protease dimerization.

Inhibition of Protease Dimerization by Non-peptidyl and Peptidyl Compounds—After establishing the validity of the FRET-HIV-1 assay to detect protease dimerization inhibition, we evaluated various newly generated non-peptidyl small molecule agents, including the currently available anti-HIV-1 drugs for their ability to inhibit protease dimerization in a blind manner, where agents examined were identified only under code in conducting the FRET-HIV-1 assay. Six different non-peptidyl small molecule agents (GRL-0036A, GRL-06579A (26), TMC126 (33), GRL-98065 (36), DRV (24), and brecaonavir (BCV) (37); M_r , ranging from 547 to 704 (Fig. 3)) were found to disrupt protease

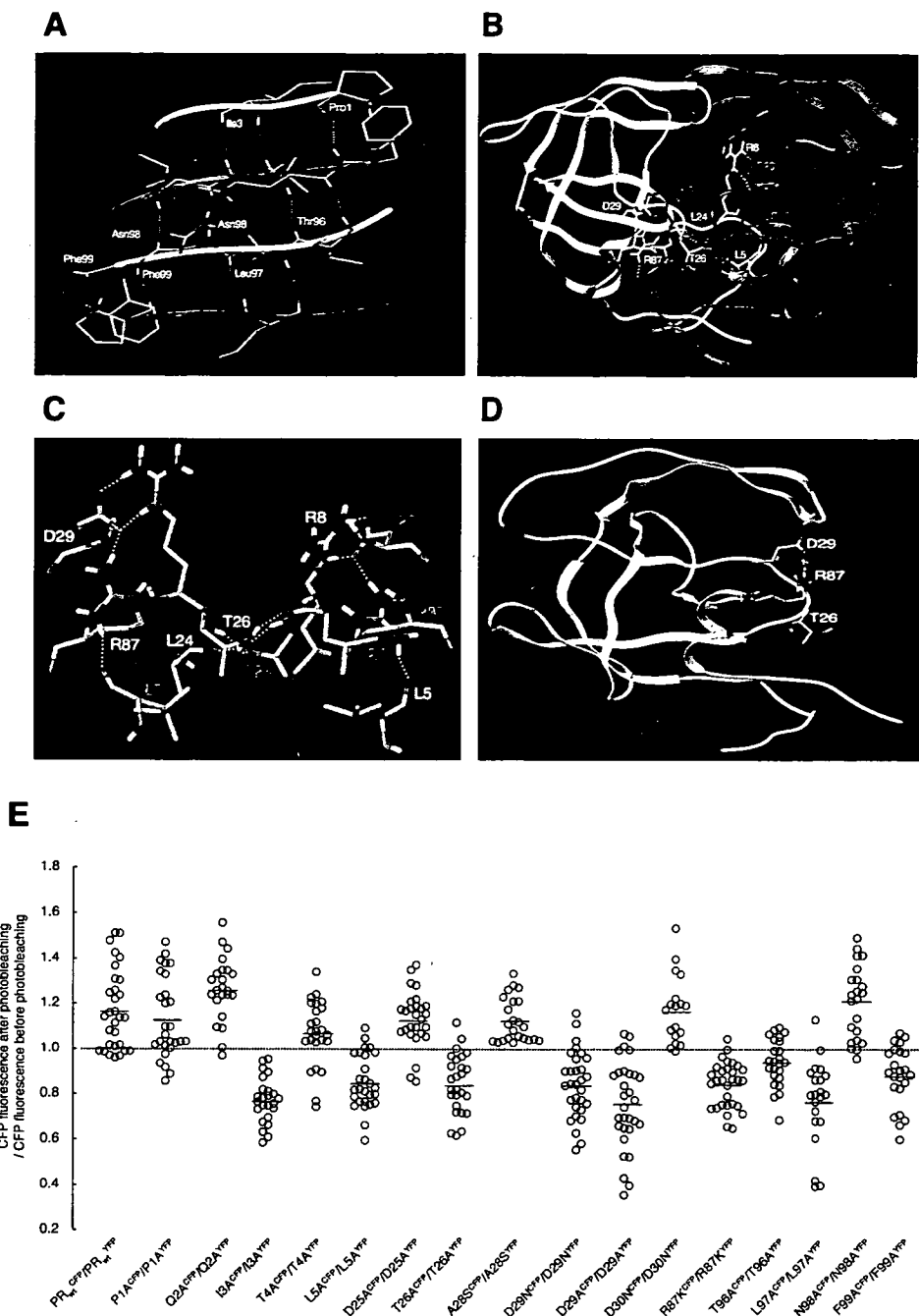


FIGURE 2. Critical amino acid residues for protease dimerization. A, four antiparallel β -sheets involving the N and C termini of both monomer subunits. Two HIV-1 protease monomer subunits are connected by four antiparallel β -sheets involving the N and C termini of both monomer subunits. It is of note that mature dimerized protease has as many as 12 hydrogen bonds in this N- and C-terminal region, and these interactions seem to be critical for dimer formation. A monomer subunit is shown by the *green ribbon*, and the other monomer subunit is shown by the *red ribbon*. A molecule disrupting these inter-protease hydrogen bond contacts can also disrupt their dimerization. B and C, intermolecular hydrogen bonds between two HIV-1 protease monomer subunits. The figure shows the intermolecular hydrogen bonds between two protease monomer subunits. The hydrogen bond interactions between protease monomer A (shown as *green ribbon*) and monomer B (shown in *red ribbon*) are Asp-29 to Arg-8', Arg-87 to Leu-5', Leu-24 to Thr-26', and Thr-26 to Thr-26'. The corresponding amino acids of monomer B also form hydrogen bonds with monomer A (i.e. Asp-29' to Arg-8, etc.). Intra-molecular hydrogen bond interaction between Asp-29 and Arg-87 is shown by *white dotted lines*. The residues forming critical intermolecular contacts between two monomer subunits are shown by atom color types (C, gray; N, blue; O, red; and H, white). Only polar hydrogens are shown. The residues of chain A are labeled *green*, and those of chain B are labeled *red*. This provides a structural explanation to the FRET experimental data, which show that mutations Leu-5, Asp-29, Thr-26, and Arg-87 prevent formation of a protease dimer. D, potential binding sites of the small molecule dimerization inhibitors. The figure shows one of the potential binding sites of the dimerization inhibitors. Asp-29, Arg-87, and Thr-26 are spatially close enough to form binding interactions with the dimerization inhibitor and prevent the other protease monomer from interacting with these residues. E, changes in emission intensity ratios upon amino acid substitution. COS7 cells were co-transfected with a pair of HIV-PR^{CFP} and HIV-PR^{YFP} carrying wild-type protease or protease with one amino acid substitution, and CFP^{A/B} ratios were determined. The CFP^{A/B} ratio value for PR_{WT}^{CFP}/PR_{WT}^{YFP} was 1.17 ± 0.18 (mean \pm 1 S.D.); PR_{P1A}^{CFP}/PR_{P1A}^{YFP}, 1.13 ± 0.18 ; PR_{O2A}^{CFP}/PR_{O2A}^{YFP}, 1.26 ± 0.14 ; PR_{I3A}^{CFP}/PR_{I3A}^{YFP}, 0.77 ± 0.10 ; PR_{T4A}^{CFP}/PR_{T4A}^{YFP}, 1.07 ± 0.14 ; PR_{L5A}^{CFP}/PR_{L5A}^{YFP}, 0.85 ± 0.12 ; PR_{D25A}^{CFP}/PR_{D25A}^{YFP}, 1.13 ± 0.12 ; PR_{T26A}^{CFP}/PR_{T26A}^{YFP}, 0.84 ± 0.13 ; PR_{A28S}^{CFP}/PR_{A28S}^{YFP}, 1.13 ± 0.10 ; PR_{D29N}^{CFP}/PR_{D29N}^{YFP}, 0.84 ± 0.15 ; PR_{D29A}^{CFP}/PR_{D29A}^{YFP}, 0.76 ± 0.19 ; PR_{D30N}^{CFP}/PR_{D30N}^{YFP}, 1.17 ± 0.15 ; PR_{R87K}^{CFP}/PR_{R87K}^{YFP}, 0.84 ± 0.10 ; PR_{T96A}^{CFP}/PR_{T96A}^{YFP}, 0.94 ± 0.10 ; PR_{L97A}^{CFP}/PR_{L97A}^{YFP}, 0.77 ± 0.19 ; PR_{N98A}^{CFP}/PR_{N98A}^{YFP}, 1.21 ± 0.16 ; and PR_{F99A}^{CFP}/PR_{F99A}^{YFP}, 0.88 ± 0.13 . All the experiments were conducted in a blind fashion. The CFP^{A/B} ratio that is >1 signifies a protease dimer, whereas a ratio that is <1 signifies disruption of protease dimerization. Note that the residue (such as Ile-3 or Asp-29) whose mutation resulted in disruption of dimerization had an inter-molecular hydrogen bond contact with the other protease monomer as shown in A–C. The mean value of the ratios is shown as *bars*.

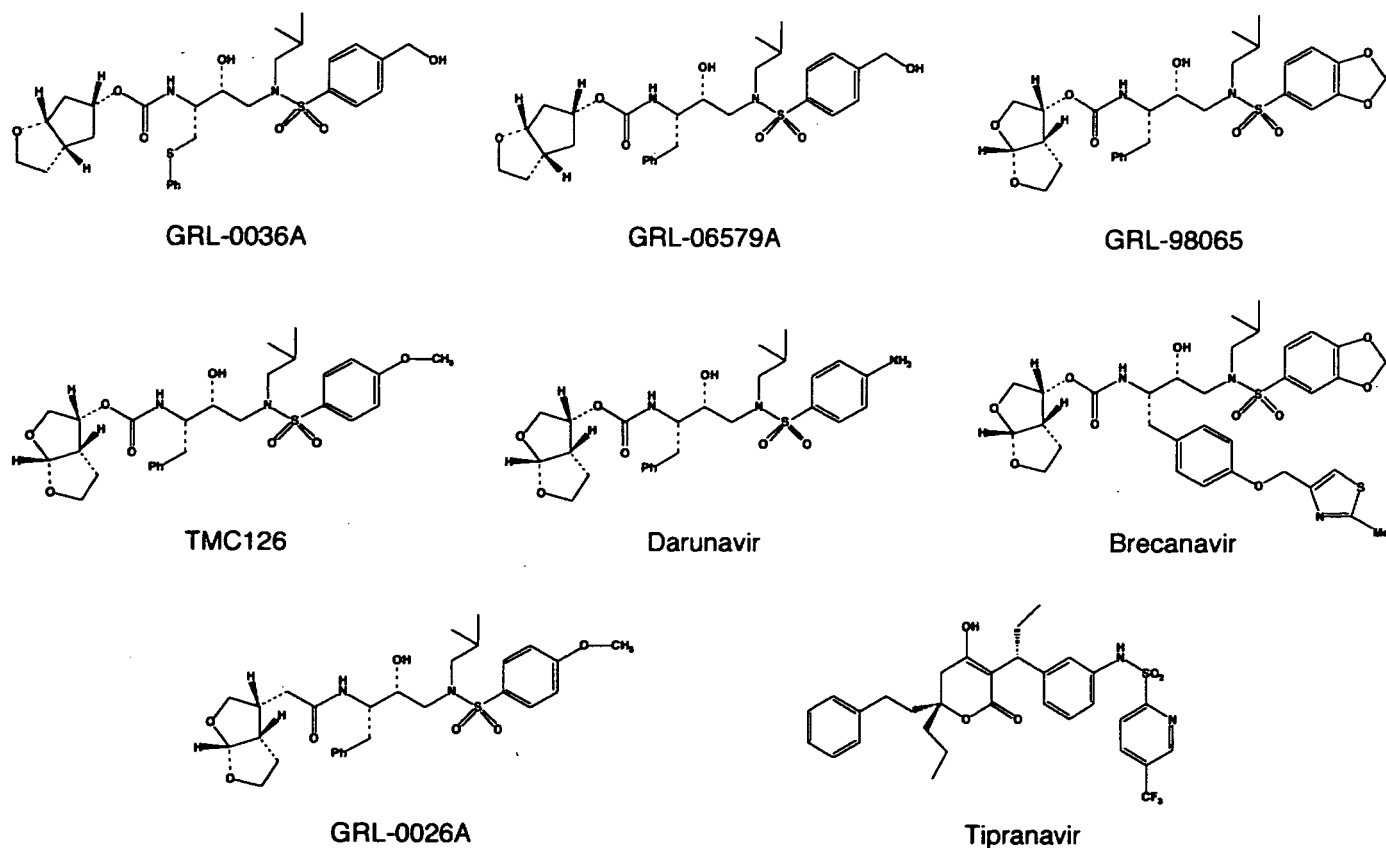


FIGURE 3. Structures of dimerization inhibitors identified. Structures of eight dimerization inhibitors are shown. The IC_{50} values for activity against HIV-1 in acute HIV-1 infection assays are shown in Table 1.

dimerization at concentration of $1 \mu\text{M}$ in the assay (Fig. 4A). All of these agents had potent inhibitory activity against HIV-1 protease with K_i values of 29, 3.5, 10, 14, 16, and $6.8 \mu\text{M}$, respectively, as examined in the assay previously described (25, 26), and were highly potent against HIV-1_{LAI} in acute HIV-1 infection assays using target $CD4^+$ MT-2 cells (24) with IC_{50} values of 0.0002 – $0.005 \mu\text{M}$ (Table 1). In addition to small molecule agents, we examined various peptides in the FRET-HIV-1 assay. A 27-amino acid peptide containing the dimer interface sequences amino acids 1–5 and amino acids 95–99 (P27: PQITLRKKRRRQRRRPPQVSFNFATLNF), which blocks HIV-1 infectivity and replication (14), also inhibited protease dimerization as examined in the FRET-HIV-1 expression assay. Another peptide P9 (RKKRRRQRRRPPQVSFNF) that lacks the dimer interface sequences and is not active against HIV-1 (14) failed to inhibit protease dimerization in the FRET-HIV-1 assay. These data again corroborated the utility of the assay to evaluate protease dimerization.

To test the robustness and reproducibility of the FRET-HIV-1 assay data, we determined the $CFP^{A/B}$ ratios in a total of 143 COS7 cells transfected with pPR_{WT}^{CFP} and pPR_{WT}^{YFP} plasmids and cultured in the presence or absence of $1 \mu\text{M}$ DRV for 3 days on 11 different occasions. In the presence of DRV, only 7 (4.9%) of 143 cells had the ratios of slightly more than 1.0, whereas all the rest (95.1%) had values of <1.0 ($n = 143$; average of 0.73 ± 0.22) (Fig. 4B). The $CFP^{A/B}$ ratios determined in the absence of DRV were mostly >1.0 ($n = 172$, average of 1.21 ± 0.17). We next examined whether a dose response in the dimer-

ization inhibition could be seen when the cells were exposed to various concentrations of DRV. As shown in Fig. 4C, DRV effectively inhibited protease dimerization at concentrations of $0.1 \mu\text{M}$ and above, whereas the average $CFP^{A/B}$ ratio was slightly >1.0 at $0.01 \mu\text{M}$, and no dimerization inhibition was seen at $0.001 \mu\text{M}$. These data show that the inhibition by DRV was roughly dose-responsive up to $0.1 \mu\text{M}$. In addition, we examined a TMC126-congener GRL-0026A (Fig. 3) that is substantially less potent than TMC126 against HIV-1 with IC_{50} of $0.48 \mu\text{M}$ (Table 1), along with TMC126 and BCV for their dose response dimerization inhibition in the FRET-HIV-1 assay and found that the inhibition was similarly dose-responsive (Fig. 4D).

None of the FDA-approved Anti-HIV-1 Drugs Except TPV Blocks Dimerization—We asked whether other currently approved PIs blocked protease dimerization in the FRET-HIV-1 assay. None of the seven PIs (saquinavir, nelfinavir, amprenavir, indinavir, ritonavir, lopinavir, and atazanavir) inhibited protease dimerization at $1 \mu\text{M}$ concentration, whereas the control DRV clearly inhibited the dimerization as shown in Fig. 4E. Considering that DRV is generally more potent against HIV-1 *in vitro* than most currently existing PIs (24), four PIs (saquinavir, amprenavir, nelfinavir, and atazanavir) were examined in the FRET-HIV-1 assay at a higher concentration, $10 \mu\text{M}$, however, none of these four PIs inhibited protease dimerization (Fig. 4F). Interestingly, TPV, which has been shown to provide more favorable virological and immunological responses in patients who have received extensive previous antiretroviral treatment than an optimized background regimen when

Potent HIV-1 Inhibition and Protease Dimerization Inhibition

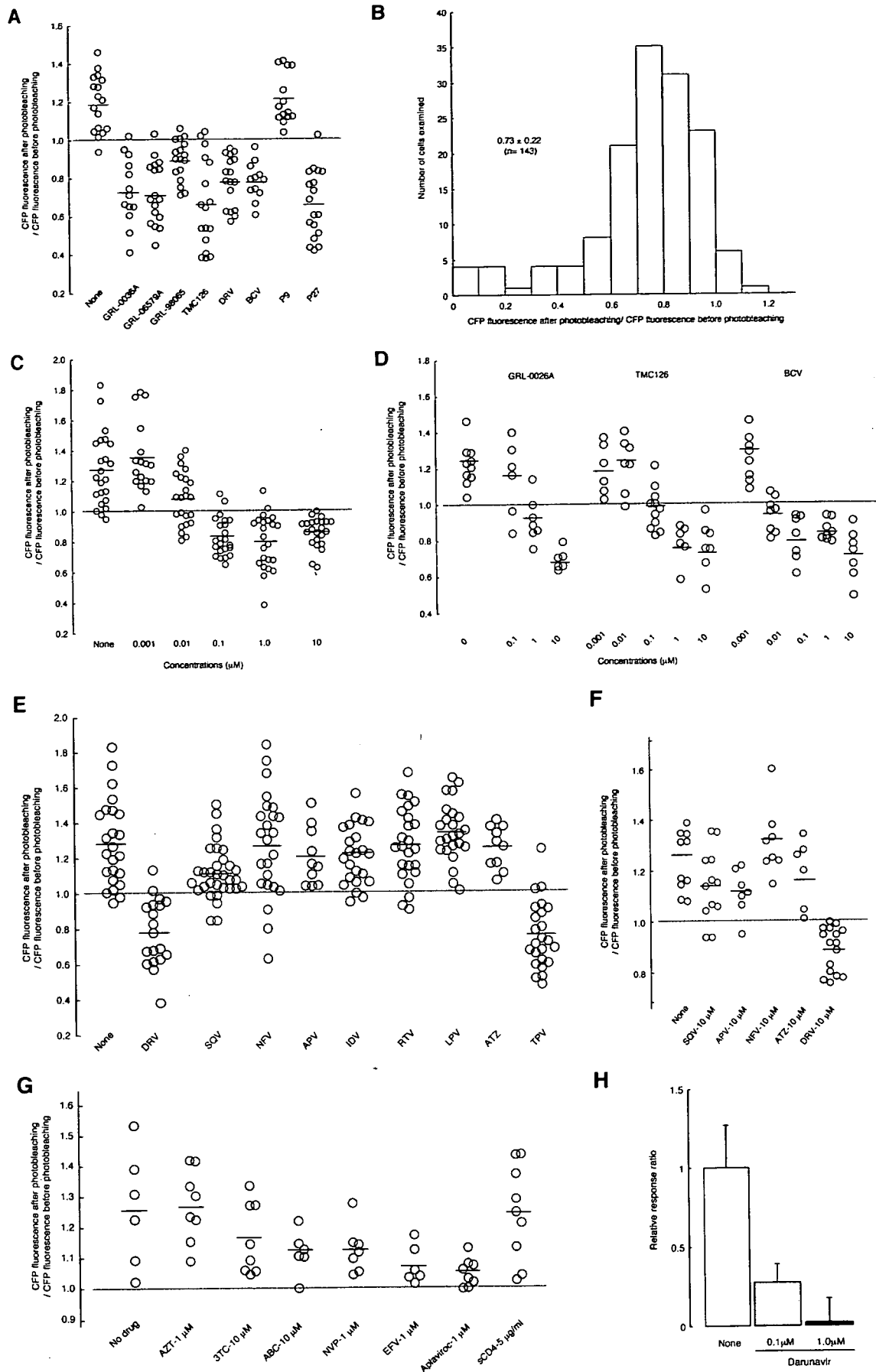


TABLE 1

Antiviral activity and enzyme inhibition of protease dimerization inhibitors

MT-2 cells (2×10^3) were exposed to 100 50% tissue culture infectious dose values of HIV-1_{LAI} and cultured in the presence of various concentrations of each drug, and the IC₅₀ values were determined using the 3-(4,5-dimethylthiazol-2-yl)-2,5-diphenyltetrazolium bromide assay. All assays were conducted in duplicate, and the data shown represent mean values (± 1 S.D.) derived from the results of three independent experiments. The chromogenic substrate Lys-Ala-Arg-Val-Nle-pnitroPhe-Glu-Ala-Nle-amide was used to determine the kinetic parameters. The K_i values were obtained from the IC₅₀ values estimated from an inhibitor dose-response curve with the spectroscopic assay using the equation $K_i = (IC_{50} - [E]/2)/(1 + [S]/K_m)$, where [E] and [S] are the PR and substrate concentrations, respectively. The K_i values were measured at four to five substrate concentrations. The measurement was repeated at least three times to produce the average values.

Drug	IC ₅₀	K _i
	μM	μM
GRL-0036A	0.005 \pm 0.002	29
GRL-06579A	0.0014 \pm 0.0008	3.5
GRL-98065	0.0004 \pm 0.0001	14
TMC126	0.0003 \pm 0.0001	10
DRV	0.0034 \pm 0.0005	16
BCV	0.0002 \pm 0.0001	6.8
GRL-0026A	0.48 \pm 0.04	ND ^a
TPV	0.10 \pm 0.04	ND

^a ND, not determined.

administered with ritonavir (38), also blocked protease dimerization (Fig. 4E).

We also examined various nucleoside and non-nucleoside reverse transcriptase inhibitors (zidovudine, lamivudine, abacavir, nevirapine, and efavirenz) as well as CCR5 inhibitor aplaviroc (39) for dimerization inhibition. However, none of these anti-HIV-1 agents showed inhibition of dimerization even at relatively higher concentrations of 1–10 μM . Soluble CD4 (5 $\mu g/ml$) also failed to inhibit protease dimerization (Fig. 4G).

Darunavir Blocks Protease Dimerization as Examined in Dual Luciferase Assay—We also established a dual luciferase assay using the CheckMate™ Mammalian Two-Hybrid System to examine whether DRV blocked protease dimerization in a different assay system. We generated pACT-PR_{WT}, producing PR_{WT}, whose N terminus is connected to the herpes simplex virus VP16 activation domain, and pBIND-PR_{WT}, producing PR_{WT}, whose N terminus is connected to GAL4 DNA-binding domain. In this system, interactions between two different PR_{WT} result in an increase in firefly luciferase expression produced by the pG5luc vector. In addition, the pBIND vector expresses Renilla luciferase under the control of the SV40 promoter, allowing the user to normalize for the differ-

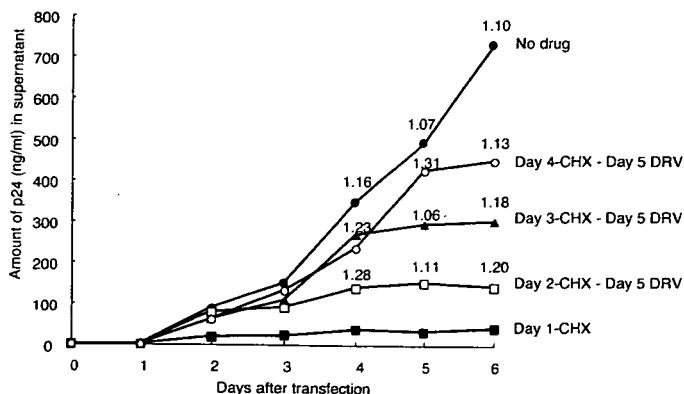


FIGURE 5. Darunavir does not dissociate once-dimerized protease in cells producing infectious HIV-1 virions. COS7 cells were co-transfected with two plasmids, pPR_{WT}^{CFP} and pPR_{WT}^{YFP}, exposed to CHX (50 $\mu g/ml$) in 24, 48, 72, and 96 h of culture. The cells were exposed to DRV on day 5 of culture. The production of HIV-1 was monitored every 24 h by determining levels of p24 Gag protein produced into culture medium. The values of the CFP^{A/B} ratio were determined at various time points.

ences in transfection efficiency. Thus, when VP16 and GAL4 closely interact upon protease dimerization, the ratio of the intensity of Fluc over that of Rluc increases, and its decrease indicates the disruption of protease dimerization. As shown in Fig. 4H, in the presence of 0.1 and 1 μM of DRV, the relative response ratios significantly decreased, further corroborating that DRV blocks protease dimerization.

Darunavir Does Not Dissociate Once-dimerized Protease in Cells Producing Infectious HIV-1 Virions—Finally, an attempt was made to determine if dimerization inhibitors could dissociate mature protease that had already dimerized. COS7 cells were co-transfected with a pair of plasmids encoding HIV-PR_{WT}^{CFP} and HIV-PR_{WT}^{YFP} and exposed to a protein synthesis inhibitor CHX (50 $\mu g/ml$) at 24, 48, 72, and 96 h of culture. The cells were then exposed to DRV on day 5 of culture, the production of HIV-1 was monitored every 24 h by determining levels of p24 Gag protein produced into culture medium, and the values of the CFP^{A/B} ratio were determined at various time points (Fig. 5). When the cells were treated with CHX on day 1 and throughout the rest of the culture period, only a small amount of p24 Gag protein production was seen but no cells emitting fluorescence were observed. When the cells were exposed to CHX on day 2 and beyond, Gag protein production was readily

FIGURE 4. Inhibition of protease dimerization. A, inhibition of protease dimerization by non-peptidyl and peptidyl compounds. COS7 cells were exposed to each of the agents (1 μM of GRL-0036A, GRL-06579A, GRL-98065, TMC126, DRV, and BCV and 10 μM of P9 and P27) and subsequently co-transfected with pPR_{WT}^{CFP} and pPR_{WT}^{YFP}. After 72 h, cultured cells were examined in the FRET-HIV-1 assay system using confocal microscopy Fluoview FV500 confocal laser scanning microscope, and CFP^{A/B} ratios were determined and plotted. The mean of these ratios obtained are shown as bars. B, distribution of the values of CFP^{A/B} ratio in the presence of 1 μM DRV. 143 cells obtained from 11 independent assays were examined, and CFP^{A/B} ratios determined were plotted. All the assays were conducted in a blinded manner. C, dose-responsive dimerization inhibition by DRV. COS7 cells were exposed to various concentrations of DRV, co-transfected with pPR_{WT}^{CFP} and pPR_{WT}^{YFP}, and A/B ratios were determined. D, dose-responsive dimerization inhibition by various non-peptidyl compounds. COS7 cells were exposed to various concentrations of GRL-0026A, TMC126, and BCV, co-transfected with pPR_{WT}^{CFP} and pPR_{WT}^{YFP}, and cultured for 72 h. At the end of the culture, CFP^{A/B} ratio values were determined. E, failure of seven clinically available protease inhibitors except DRV and TPV to inhibit the dimerization of PR_{WT}^{CFP} and PR_{WT}^{YFP}. COS7 cells were co-transfected with pPR_{WT}^{CFP} and pPR_{WT}^{YFP} in the presence of various anti-HIV-1 protease inhibitors at concentration of 1 μM , and A/B ratios were determined. F, failure of a high concentration of four clinically available protease inhibitors to inhibit HIV-1 protease dimerization. COS7 cells were co-transfected with pPR_{WT}^{CFP} and pPR_{WT}^{YFP} in the presence of four PIs (saquinavir, amprenavir, nelfinavir, and atazanavir) at a higher concentration of 10 μM , cultured for 72 h, and CFP^{A/B} ratios were determined. Note that all the CFP^{A/B} ratio values were >1.0 except for those of DRV. G, various approved anti-HIV-1 agents failed to inhibit HIV-1 protease dimerization. COS7 cells were co-transfected with pPR_{WT}^{CFP} and pPR_{WT}^{YFP} in the presence of various nucleoside and non-nucleoside reverse transcriptase inhibitors (zidovudine, lamivudine, abacavir, nevirapine, and efavirenz), CCR5 inhibitor aplaviroc, and soluble CD4, and A/B ratios were determined. H, protease dimerization inhibition by DRV on dual luciferase assay. COS7 cells were co-transfected with pACT-PR_{WT}, pBIND-PR_{WT}, and pG5luc in the presence or absence of 0.1 or 1.0 μM of DRV, cultured for 48 h, and the intensity of firefly luminescence (Fluc) and Renilla luminescence (Rluc) was measured with TR717 microplate luminometer. DRV was added to the culture medium simultaneously with plasmids to be used. Fluc/Rluc intensity ratios were determined with co-transfection of pACT-PR_{WT}, pBIND-PR_{WT}, and pG5luc in the absence of DRV, serving as maximal values.

Potent HIV-1 Inhibition and Protease Dimerization Inhibition

detected by day 2, but no significant increment in the production of p24 Gag protein was seen on those days subsequent to the addition of CHX. When the cells were exposed to CHX on days 3 and 4, greater amounts of Gag protein were seen (Fig. 5). The CFP^{A/B} ratios determined on days 4 and 5 of culture were all >1.0, signifying that HIV-1 protease had been generated and dimerization had occurred. On day 5, DRV (1 μ M) was added to all the cultures described above and the CFP^{A/B} ratios were determined on day 6 of culture. The ratios remained >1.0 in all of the cultured COS7 cells (Fig. 5). These data strongly suggest that DRV does not dissociate mature protease once dimerized within the HIV-1-producing COS7 cells.

DISCUSSION

In the present study, we developed an intermolecular FRET-based HIV-1-expression assay (FRET-HIV-1 expression assay) that employed cyan and yellow fluorescent protein-tagged HIV-1 protease monomers. Using this assay, we identified a group of non-peptidyl small molecule inhibitors of HIV-1 protease dimerization (molecular weight, 547–704). Dimerization of HIV-1 protease subunits is an essential process for the acquisition of proteolytic activity of HIV-1 protease, which plays a critical role in the replication cycle of HIV-1. Hence, the inhibition of dimerization of HIV-1 protease subunits represents a unique target for potential intervention of HIV-1 replication. The strategy to target protease dimerization as a possible anti-HIV-1 modality has been explored (8, 11–13), and certain compounds have been reported as potential protease dimerization inhibitors. However, no direct evidence of dimerization inhibition by such compounds has been documented. The present report represents the first demonstration that non-peptidic small molecule agents can disrupt protease dimerization.

The structural feature that is in common to the four dimerization inhibitors (TMC126 (33), GRL-98065 (36), DRV (24), and BCV (37)) is that all of these agents contain the structure-based designed privileged cyclic ether-derived non-peptidyl P2 ligand, 3(R),3 α (S),6 α (R)-bistetrahydrofuranylurethane (bis-THF) and a sulfonamide isostere (22, 23). GRL-0036A and GRL-06579A (26) have bis-THF-related ligand instead of bis-THF. Crystallographic data of dimerized protease complexed with three dimerization inhibitors (GRL-98065 (36), TMC126,³ and DRV (40)) have revealed that bis-THF forms three tight hydrogen bond interactions with Asp-29 and Asp-30, two highly conserved catalytic site amino acids. We also observed that TPV has the ability to disrupt protease dimerization. TPV, which does not possess the bis-THF component, also has interactions with both Asp-29 and Asp-30 through its pyridinesulfonamide group, as shown in crystallographic analysis of a dimerized protease complexed with TPV (41). Thus, the inhibition of protease dimerization is not inherent only to the bis-THF component.

Most of the dimerization inhibitors we examined in this study exerted potent activity against PI-resistant protease in addition to their potent activity to wild-type HIV-1. DRV is potent against HIV-1_{NL4-3} variants exposed to and selected for

resistance to saquinavir, indinavir, nelfinavir, and ritonavir (24). Crystal structures of HIV-1 protease with a single mutation (D30N, I50V, V82A, I84V, or L90M) complexed with DRV demonstrate that DRV not only binds to the same catalytic active site as it does for wild-type protease but also maintains hydrogen bond interactions with the backbone atoms of Asp-29 and Asp-30 (40, 42). GRL-06579A and GRL-98065 are also potent against multidrug resistant HIV-1 strains, and molecular modeling indicates that for multidrug-resistant clinical isolates, these inhibitors maintain many of the interactions to critical active site residues (26, 36). TPV, which is active against HIV-1 carrying multidrug-resistant protease, also maintains critical hydrogen bond interactions with backbone atoms in the catalytic active site of mutant protease (43).

It is of note that the D30N-carrying HIV-1 variant is infectious and replication-competent (34). Structural studies do not show any hydrogen bond interactions between two monomer proteases mediated through Asp-30, and the FRET-HIV-1 expression assay showed that D30N mutant did not disrupt protease dimerization. This suggests that Asp-30 is not a critical residue for disrupting protease dimerization, and the interaction of these inhibitors with Asp-30 is not linked to the observed dimerization inhibition. However, potential interactions of dimerization inhibitors such as DRV involving Asp-29 could be critical, because D29N and D29A mutations disrupted protease dimer formation (Fig. 2E). Our analysis using the FRET-HIV-1 expression assay also revealed that the introduction of T26A and R87K to HIV-1 protease disrupted protease dimerization (the average CFP^{A/B} ratios were all <1.0 (Fig. 2E)). If the protease monomer takes a configuration comparable to that in the dimerized protease, it is possible that the hydrogen bonding of the inhibitors with Asp-29, and/or Thr-26 and Arg-87, both of which are in the vicinity of Asp-29 and could be critical for dimerization, could be associated with the disruption of dimerization process through affecting the intermolecular and/or intramolecular hydrogen bond network (Fig. 2, B–D). In this regard, Ishima *et al.* (30) have shown that a truncated protease monomer takes a configuration similar to the one in the mature dimerized protease; however, it is unknown whether the untruncated monomer subunit takes a similar mature configuration. Furthermore, it is not known as to what stage of protease maturation (before dimerization) the dimerization inhibitors reported here bind to the monomer subunit in.

Another possible mechanism of the dimerization inhibition by the agents reported here is that they might interact with another dimerization interface formed by an interdigitation of the N- and C-terminal portions of each monomer (residues 1–5 and 95–99 (Fig. 2A)). In this regard, when we introduced a Pro-1 to Ala substitution (P1A), Q2A, I3A, T4A, L5A, T96A, L97A, N98A, or F99A into the replication-competent HIV-1_{NL4-3} five substitutions (I3A, L5A, T96A, L97A, and F99A) produced the ratios of less than 1.0, strongly suggesting that most of the protease monomer subunit failed to dimerize with each of these five substitutions. These data confirmed the five amino acids at the N terminus and those at the C terminus are critical for protease dimerization (30–32). There are no polar interactions involving Q2A or T4A, so it is not surprising that

³ Y. Koh, S. Matsumi, D. Das, M. Amano, D. A. Davis, J. Li, S. Leschenko, A. Baldrige, T. Shioda, R. Yarchoan, A. K. Ghosh, and H. Mitsuya, unpublished observation.

these mutations did not affect dimer formation. However, the failure of P1A and N98A to disrupt dimerization does not necessarily indicate that these amino acids are not critical for protease dimerization. It is possible that conversion to a residue other than alanine may disrupt dimerization.

In the present study, DRV failed to dissociate mature protease dimer (Fig. 5). It is of note that mature dimerized protease has as many as 12 hydrogen bonds in the N- and C-terminal regions, which may explain in part why DRV failed to dissociate two subunits of mature protease. These data also suggest that protease dimerization is inhibited before the association of two protease subunits occurs, probably when protease is in the form of nascent Gag-Pol polyprotein. However, the absence of structural data of nascent forms of protease subunit-containing polyprotein makes it difficult to conclusively predict how the dimerization inhibitors inhibit protease dimerization.

It is noteworthy that the D25N substitution, which is known to render HIV-1 protease enzymatically inactive (44), failed to disrupt dimerization (Fig. 2E), showing that catalytically inactive subunits are still capable of undergoing dimerization. This observation indicates that the dimerization inhibition is a differing event than the process that confers catalytic activity on two protease monomer subunits.

DRV has a potent activity against a wide spectrum of HIV-1 isolates, including highly multiprotease-inhibitor-resistant HIV-1 variants. The emergence of DRV-resistant HIV-1 seems to be substantially delayed both *in vitro* (45) and clinical settings (46, 47). One can speculate that DRV inhibits protease dimerization, leaving catalytically inert monomers, but if certain monomers escape from DRV and achieve the mature dimer form, DRV again blocks the proteolytic action of mature (wild-type and mutant) protease as a conventional protease inhibitor. This dual anti-HIV-1 function of DRV may explain why DRV is such a highly effective anti-HIV-1 therapeutic and differentiates it from many of the currently available protease inhibitors (46, 47). It is of note that the plasma concentrations of DRV achieved in those receiving DRV and ritonavir remain >2 $\mu\text{g/ml}$ or ~ 3.66 μM (48). These concentrations substantially exceed the concentration of DRV effectively disrupting protease dimerization (0.1 μM in culture as shown in Fig. 4C). Hence, the dimerization inhibition by DRV should be in operation in the clinical settings. Furthermore, DRV could more efficiently disrupt protease dimerization in individuals with HIV-1 infection receiving DRV and ritonavir, because the protease expression levels upon transfection in this study appear to be considerably greater than the protease expression levels *in vivo*, considering that the p24 production levels could be as high as 500–1500 ng/ml by 5 days following transfection of COS7 cells with plasmids used in the FRET-HIV-1 expression assay. The inhibition of HIV-1 protease dimerization by non-peptidyl small molecule agents represents a unique mechanism of HIV-1 intervention, and the dually functional inhibitors reported here might serve as potential candidates as a new class of therapeutic agents for HIV-1 infection and AIDS. The present data should not only help design and examine agents that potentially inhibit HIV-1 protease dimerization but also should give new insights into the process and dynamics of HIV-1 protease dimerization *per se*.

Acknowledgments—We thank Philip Yin and Kenji Maeda for critical reading of the manuscript, Toshikazu Miyakawa for helpful discussion, and Maki Nakayama for technical assistance.

REFERENCES

- Simon, V., and Ho, D. D. (2003) *Nat. Rev. Microbiol.* **1**, 181–190
- Carr, A. (2003) *Nat. Rev. Drug Discov.* **2**, 624–634
- Wlodawer, A., Miller, M., Jaskolski, M., Sathyanarayana, B. K., Baldwin, E., Weber, I. T., Selk, L. M., Clawson, L., Schneider, J., and Kent, S. B. (1989) *Science* **245**, 616–621
- Kohl, N. E., Emimi, E. A., Schleif, W. A., Davis, L. J., Heimbach, J. C., Dixon, R. A., Scolnick, E. M., and Sigal, I. S. (1988) *Proc. Natl. Acad. Sci. U. S. A.* **85**, 4686–4690
- Lapatto, R., Blundell, T., Hemmings, A., Overington, J., Wilderspin, A., Wood, S., Merson, J. R., Whittle, P. J., Danley, D. E., Geoghegan, K. F., Hawrylik, S. J., Lee, S. E., Scheld, K. G., and Hobart, P. M. (1989) *Nature* **342**, 299–302
- Spinelli, S., Liu, Q. Z., Alzari, P. M., Hirel, P. H., and Poljak, R. J. (1991) *Biochimie (Paris)* **73**, 1391–1396
- Strisovsky, K., Tessmer, U., Langner, J., Konvalinka, J., and Krausslich, H. G. (2000) *Protein Sci.* **9**, 1631–1641
- Levy, Y., Caflish, A., Onuchic, J. N., and Wolynes, P. G. (2004) *J. Mol. Biol.* **340**, 67–79
- Levy, Y., and Caflish, A. (2003) *J. Phys. Chem. B* **107**, 3068–3079
- Todd, M. J., Semo, N., and Freire, E. (1998) *J. Mol. Biol.* **283**, 475–488
- Bowman, M. J., Byrne, S., and Chmielewski, J. (2005) *Chem. Biol.* **12**, 439–444
- Frutos, S., Rodriguez-Mias, R. A., Madurga, S., Collinet, B., Reboud-Ravaux, M., Ludevid, D., and Giralt, E. (2007) *Biopolymers* **88**, 164–173
- Bannwarth, L., Kessler, A., Pethe, S., Collinet, B., Merabet, N., Boggetto, N., Sicsic, S., Reboud-Ravaux, M., and Ogeri, S. (2006) *J. Med. Chem.* **49**, 4657–4664
- Davis, D. A., Brown, C. A., Singer, K. E., Wang, V., Kaufman, J., Stahl, S. J., Wingfield, P., Maeda, K., Harada, S., Yoshimura, K., Kosalaraksa, P., Mitsuya, H., and Yarchoan, R. (2006) *Antiviral Res.* **72**, 89–99
- Hoess, R. H., and Abremski, K. (1984) *Proc. Natl. Acad. Sci. U. S. A.* **81**, 1026–1029
- Fang, G., Weiser, B., Visosky, A., Moran, T., and Burger, H. (1999) *Nat. Med.* **5**, 239–242
- Gatanaga, H., Suzuki, Y., Tsang, H., Yoshimura, K., Kavlick, M. F., Nagashima, K., Gorelick, R. J., Mardy, S., Tang, C., Summers, M. F., and Mitsuya, H. (2002) *J. Biol. Chem.* **277**, 5952–5961
- Sekar, R. B., and Periasamy, A. (2003) *J. Cell Biol.* **160**, 629–633
- Bastiaens, P. I., Majoul, I. V., Verveer, P. J., Soling, H. D., and Jovin, T. M. (1996) *EMBO J.* **15**, 4246–4253
- Bastiaens, P. I., and Jovin, T. M. (1996) *Proc. Natl. Acad. Sci. U. S. A.* **93**, 8407–8412
- Szczesna-Skorupa, E., Mallah, B., and Kemper, B. (2003) *J. Biol. Chem.* **278**, 31269–31276
- Ghosh, A. K., Pretzer, E., Cho, H., Hussain, K. A., and Duzgunes, N. (2002) *Antiviral Res.* **54**, 29–36
- Ghosh, A. K., Leshchenko, S., and Noetzel, M. (2004) *J. Org. Chem.* **69**, 7822–7829
- Koh, Y., Nakata, H., Maeda, K., Ogata, H., Bilcer, G., Devasamudram, T., Kincaid, J. F., Boross, P., Wang, Y. F., Tie, Y., Volarath, P., Gaddis, L., Harrison, R. W., Weber, I. T., Ghosh, A. K., and Mitsuya, H. (2003) *Antimicrob. Agents Chemother.* **47**, 3123–3129
- Kovalevsky, A. Y., Liu, F., Leshchenko, S., Ghosh, A. K., Louis, J. M., Harrison, R. W., and Weber, I. T. (2006) *J. Mol. Biol.* **363**, 161–173
- Ghosh, A. K., Sridhar, P. R., Leshchenko, S., Hussain, A. K., Li, J., Kovalevsky, A. Y., Walters, D. E., Wedekind, J. E., Grum-Tokars, V., Das, D., Koh, Y., Maeda, K., Gatanaga, H., Weber, I. T., and Mitsuya, H. (2006) *J. Med. Chem.* **49**, 5252–5261
- Maibaum, J., and Rich, D. H. (1988) *J. Med. Chem.* **31**, 625–629
- Miyawaki, A., Llopis, J., Heim, R., McCaffery, J. M., Adams, J. A., Ikura, M., and Tsien, R. Y. (1997) *Nature* **388**, 882–887

Potent HIV-1 Inhibition and Protease Dimerization Inhibition

29. Babe, L. M., Rose, J., and Craik, C. S. (1992) *Protein Sci.* **1**, 1244–1253
30. Ishima, R., Torchia, D. A., Lynch, S. M., Gronenborn, A. M., and Louis, J. M. (2003) *J. Biol. Chem.* **278**, 43311–43319
31. Ishima, R., Ghirlando, R., Tozser, J., Gronenborn, A. M., Torchia, D. A., and Louis, J. M. (2001) *J. Biol. Chem.* **276**, 49110–49116
32. Louis, J. M., Ishima, R., Nesheiwat, I., Pannell, L. K., Lynch, S. M., Torchia, D. A., and Gronenborn, A. M. (2003) *J. Biol. Chem.* **278**, 6085–6092
33. Yoshimura, K., Kato, R., Kavlick, M. F., Nguyen, A., Maroun, V., Maeda, K., Hussain, K. A., Ghosh, A. K., Gulnik, S. V., Erickson, J. W., and Mitsuya, H. (2002) *J. Virol.* **76**, 1349–1358
34. Patick, A. K., Mo, H., Markowitz, M., Appelt, K., Wu, B., Musick, L., Kalish, V., Kaldor, S., Reich, S., Ho, D., and Webber, S. (1996) *Antimicrob. Agents Chemother.* **40**, 292–297
35. Konvalinka, J., Litterst, M. A., Welker, R., Kottler, H., Rippmann, F., Heuser, A. M., and Krausslich, H. G. (1995) *J. Virol.* **69**, 7180–7186
36. Amano, M., Koh, Y., Das, D., Li, J., Leschenko, S., Wang, Y. F., Boross, P. I., Weber, I. T., Ghosh, A. K., and Mitsuya, H. (2007) *Antimicrob. Agents Chemother.* **51**, 2143–2155
37. Miller, J. F., Andrews, C. W., Brieger, M., Furfine, E. S., Hale, M. R., Hanlon, M. H., Hazen, R. J., Kaldor, I., McLean, E. W., Reynolds, D., Sammond, D. M., Spaltenstein, A., Tung, R., Turner, E. M., Xu, R. X., and Sherrill, R. G. (2006) *Bioorg. Med. Chem. Lett.* **16**, 1788–1794
38. Hicks, C. B., Cahn, P., Cooper, D. A., Walmsley, S. L., Katlama, C., Clotet, B., Lazzarin, A., Johnson, M. A., Neubacher, D., Mayers, D., and Valdez, H. (2006) *Lancet* **368**, 466–475
39. Maeda, K., Nakata, H., Koh, Y., Miyakawa, T., Ogata, H., Takaoka, Y., Shibayama, S., Sagawa, K., Fukushima, D., Moravek, J., Koyanagi, Y., and Mitsuya, H. (2004) *J. Virol.* **78**, 8654–8662
40. Tie, Y., Boross, P. I., Wang, Y. F., Gaddis, L., Hussain, A. K., Leshchenko, S., Ghosh, A. K., Louis, J. M., Harrison, R. W., and Weber, I. T. (2004) *J. Mol. Biol.* **338**, 341–352
41. Thaisrivongs, S., Skulnick, H. I., Turner, S. R., Strohbach, J. W., Tommasi, R. A., Johnson, P. D., Aristoff, P. A., Judge, T. M., Gammill, R. B., Morris, J. K., Romines, K. R., Chrusciel, R. A., Hinshaw, R. R., Chong, K. T., Tarp-ley, W. G., Poppe, S. M., Slade, D. E., Lynn, J. C., Horng, M. M., Tomich, P. K., Seest, E. P., Dolak, L. A., Howe, W. J., Howard, G. M., Schwende, F. J., Toth, L. N., Padbury, G. E., Wilson, G. J., Shiou, L., Zipp, G. L., Wilkinson, K. F., Rush, B. D., Ruwart, M. J., Koeplinger, K. A., Zhao, Z., Cole, S., Zaya, R. M., Kakuk, T. J., Janakiraman, M. N., and Watenpaugh, K. D. (1996) *J. Med. Chem.* **39**, 4349–4353
42. Kovalevsky, A. Y., Tie, Y., Liu, F., Boross, P. I., Wang, Y. F., Leshchenko, S., Ghosh, A. K., Harrison, R. W., and Weber, I. T. (2006) *J. Med. Chem.* **49**, 1379–1387
43. Muzammil, S., Armstrong, A. A., Kang, L. W., Jakalian, A., Bonneau, P. R., Schmelmer, V., Amzel, L. M., and Freire, E. (2007) *J. Virol.* **81**, 5144–5154
44. Prabu-Jeyabalan, M., Nalivaika, E. A., Romano, K., and Schiffer, C. A. (2006) *J. Virol.* **80**, 3607–3616
45. De Meyer, S., Azijn, H., Surleraux, D., Jochmans, D., Tahri, A., Pauwels, R., Wigerinck, P., and de Bethune, M. P. (2005) *Antimicrob. Agents Chemother.* **49**, 2314–2321
46. Poveda, E., Blanco, F., Garcia-Gasco, P., Alcolea, A., Briz, V., and Soriano, V. (2006) *AIDS* **20**, 1558–1560
47. Youle, M., Staszweski, S., Clotet, B., Arribas, J. R., Blaxhult, A., Carosi, G., Dejesus, E., Di Perri, G., Estrada, V., Fisher, M., Kovacs, C., Kulasegaram, R., Lazzarin, A., Marriott, D., Munoz, L., Reynes, J., Shalit, P., Slim, J., Tsoukas, C., Vaccaro, A., and Vera, J. (2006) *HIV Clin. Trials* **7**, 86–96
48. Hoetelmans, R., Van der Sandt, I., De Pauw, M., Struble, K., Peeters, M., and Van der Geest, R. (2003) *10th Conference on Retroviruses and Opportunistic Infections*, Boston, February 10–14, 2003, Abstr. 549, Foundation for Retrovirology and Human Health, Alexandria, VA

Polymorphisms in CCR5 chemokine receptor gene in Japan

H. Liu,*† E. E. Nakayama,* I. Theodorou,‡ Y. Nagai,§ S. Likanonsakul,¶ C. Wasi,** P. Debre,‡ A. Iwamoto†† & T. Shioda*

Summary

Mutations in the human CC chemokine receptor 5 (*CCR5*) gene may alter the expression or function of the protein product, thereby altering chemokine binding/signalling or human immunodeficiency virus type 1 (HIV-1) infection of the cells that normally express *CCR5* protein. We performed a systematic survey of natural sequence variations in an 8.1-kb region of the entire *CCR5* gene as well as *CCR2V64I* in 50 Japanese subjects and evaluated the effects of those variations on *CCR5* promoter activity. We also analysed *CCR5* promoters and *CCR2V64I* in 80 more Japanese and 186 Thais. There was no 32-bp deletion observed in Caucasians, but two types of non-synonymous substitutions were found in *CCR5* genes of Japanese. Our results showed several novel characteristics of the *CCR2-CCR5* haplotype structure that were not reported from studies on Caucasians and African-Americans. Specifically, we were able to show that the G allele at position -2852 from the *CCR5* open reading frame in Japanese and Thais is the representative of the *CCR5* promoter haplotype that was reported to be associated with rapid progression to acquired immune deficiency syndrome (AIDS) in HIV-1-infected individuals. Furthermore, nearly all non-synonymous polymorphisms in Japanese *CCR5* occurred in haplotypes with elevated promoter activity. We thus hypothesized that there was a certain selective pressure favouring low levels of *CCR5* expression during human evolution.

Introduction

Human CC chemokine receptor 5 (*CCR5*) mediates the activation of cells by the CC chemokines macrophage inflammatory protein-1 α and -1 β (MIP-1 α or CCL3, and MIP-1 β or CCL4), and regulated on activation normal T cells expressed and secreted (RANTES or CCL5). Identification of *CCR5* as an essential co-receptor for the cellular entry of human immunodeficiency virus type 1 (HIV-1) R5 strains (Alkhatib *et al.*, 1996; Deng *et al.*, 1996; Dragic *et al.*, 1996; Feng *et al.*, 1996), which is preferentially transmitted between individuals (Zhu *et al.*, 1993), has led to many studies on *CCR5* and its ligands. Mutations in the *CCR5* gene may alter the expression or function of the protein product, thereby altering chemokine binding/signalling or HIV-1 infection of the cells that normally express the *CCR5* protein. Indeed, a 32-base pair (bp) deletion in the *CCR5* coding region (*CCR5* Δ 32), which results in a premature termination codon, confers marked resistance to HIV-1 infection in homozygotes (Liu *et al.*, 1996; Samson *et al.*, 1996), and delays progression to AIDS and death by 2–3 years in patients heterozygous for this allele (Dean *et al.*, 1996; Huang *et al.*, 1996). The delayed progression to AIDS and death in individuals heterozygous for *CCR5* Δ 32 has been attributed to reduced cell surface expression of *CCR5* (Wu *et al.*, 1997), which is speculated to result in a slower rate of replication and spread of the virus. Although heterozygosity for *CCR5* Δ 32 is associated with a small reduction in surface expression of *CCR5*, cells from individuals with the wild-type *CCR5* genotype showed a wide range in surface expression (Wu *et al.*, 1997), raising the possibility that polymorphisms, other than *CCR5* Δ 32, exert significant effects on *CCR5* expression. For example, the much more rarely occurring *CCR5* *m303A* is a nonsense mutation of the *CCR5* coding region that exerts effects similar to those of *CCR5* Δ 32 (Quillent *et al.*, 1998). Moreover, Asian-specific *CCR5* 893(-) is a single-nucleotide deletion in the *CCR5* coding region, and the levels of *CCR5* expression on the surface of CD4 positive cells are greatly reduced in individuals bearing this allele (Shioda *et al.*, 2001). The *CCR2* mutation, *CCR2* 64I, which is in strong linkage disequilibrium with another mutation *CCR5* -1835T (*CCR5* 927T in numbering system C, see Materials and Methods for definitions of numbering systems A, B, and C) in the second intron of the *CCR5*

* Department of Viral Infections, Research Institute for Microbial Diseases, Osaka University, Osaka, Japan, † Miller School of Medicine, University of Miami, Miami, FL, USA, ‡ Hôpital Pitié SalPetrière et INSERM UR543 Bâtiment CERVI, Paris, France, § Center of Research Network for Infectious Diseases, Riken, Yokohama, Japan, ¶ Bamrasnaradura Institute, Nonthaburi, Thailand, ** Department of Microbiology, Faculty of Medicine Siriraj Hospital, Mahidol University, Bangkok, Thailand and †† Division of Infectious Diseases, Institute of Medical Science, University of Tokyo, Tokyo, Japan

Authors H. Liu and E. E. Nakayama contributed equally to this work.

Received 5 May 2007; revised 5 May 2007; accepted 17 May 2007

Correspondence: Tatsuo Shioda, Department of Viral Infections, Research Institute for Microbial Diseases, Osaka University, 3-1 Yamada-oka, Suita, Osaka 565-0871, Japan. Tel: +81 6 6879 8346; Fax: +81 6 6879 8347; E-mail: shioda@biken.osaka-u.ac.jp